2007

Results from the DC-8 Inlet Characterization Experiment (DICE): Airborne Versus Surface Sampling of Mineral Dust and Sea Salt Aerosols

Cameron S. McNaughton
University of Hawaii, csmcnaug@hawaii.edu

Antony D. Clarke
University of Hawaii, tclarke@soest.hawaii.edu

Steven G. Howell
University of Hawaii

Mitchell Pinkerton
University of Hawaii

Bruce Anderson
NASA Langley Research Center, Hampton, Virginia, USA

See next page for additional authors

Aerosol Science and Technology, 41:136–159, 2007

ISSN: 0278-6826 print / 1521-7388 online
DOI: 10.1080/02786820601118406

Results from the DC-8 Inlet Characterization Experiment (DICE): Airborne Versus Surface Sampling of Mineral Dust and Sea Salt Aerosols

Cameron S. McNaughton,[1] Antony D. Clarke,[1] Steven G. Howell,[1] Mitchell Pinkerton,[1] Bruce Anderson,[2] Lee Thornhill,[3] Charlie Hudgins,[3] Edward Winstead,[4] Jack E. Dibb,[5] Eric Scheuer,[5] and Hal Maring[6]

[1]*School of Ocean and Earth Science and Technology, University of Hawai'i, Honolulu, Hawaii, USA*
[2]*NASA Langley Research Center, Hampton, Virginia, USA*
[3]*SAIC, Hampton, Virginia, USA*
[4]*GATS, Inc, Hampton, Virginia, USA*
[5]*Institute for the Study of Earth, Oceans, and Space, University of New Hampshire, Durham, New Hampshire, USA*
[6]*NASA Headquarters, Washington, DC, USA*

During May and June of 2003 NASA conducted the DC-8 Inlet Characterization Experiment (DICE). The study was undertaken to quantify the performance of three passive, solid diffuser inlets used aboard the DC-8 aircraft to sample optically effective aerosol sizes. Aerosol optical properties measured behind the University of Hawai'i (UH) and the University of New Hampshire (UNH) inlets were within 10% of the ground based measurements whereas the NASA Langley (LaRC) inlet reduced scattering values for supermicrometer dust by approximately 50%. Based on the DICE results the aerodynamic 50% passing efficiency of the inlets and transport plumbing is determined to be above 5.0 and 4.1 μm for the UH and UNH inlets and 3.6 μm for the LaRC inlet. These aerodynamic sizes correspond to geometric particle diameters of 3.1, 2.5, and 2.0 μm ignoring shape factor and assuming particle densities of 2.6 g cm^{-3}. Sea salt aerosols sampled at high relative humidity revealed that the UH and the UNH inlets performed nearly identically in the marine environment. Aerosol optical properties measured behind the UH inlet were within 30% of measurements made at the NOAA/ESRL Trinidad Head Observatory and in some cases were better than 10%. We conclude that quantitative measurements of optical properties and processes linked to aerosol surface chemistry can be effectively studied aboard the NASA DC-8 using the UH and UNH inlets because aerosol particles less than 4 μm in aerodynamic diameter typically dominate aerosol optical properties and surface area.

Received June 20, 2006; accepted November 14, 2006.

The authors would like to thank Dr. John Ogren, Betsy Andrews, and Michael Ives from the NOAA/ESRL Aerosol Group for maintaining the Trinidad Head Observatory and for providing the relevant data. We would also like to thank the DC-8 mission managers and ground crew from NASA's Dryden Flight Research Center. This research was conducted under NASA Grants: NCC-1-416 and NNG-04-GB-396 with additional support from NASA's Earth System Science Fellowship, NNG-05-GQ-45H. This is SOEST publication number 7005.

Address correspondence to Cameron McNaughton, Department of Oceanography, University of Hawaii, 1000 Pope Road, Honolulu, HI 96822, USA. E-mail: csmcnaug@hawaii.edu

INTRODUCTION

Sea-salt and mineral dusts are primary aerosols generated mechanically during air-sea interactions and land surface processes (i.e., aeolian erosion). Though low in particle number, these aerosols can dominate the aerosol surface area and volume distributions and on a mass basis have the highest global emission rate (Tg yr^{-1}) of all aerosol species (Raes et al. 2000). Despite the vast surface area of the world ocean, the effective removal of sea salt aerosols by wet deposition typically confines these aerosols to the marine boundary layer (MBL). Mineral dust from the Sahara (Haywood et al. 2001; Reid et al. 2003a; Reid et al. 2003b), from Asia (Clarke et al. 2001; Husar et al. 2001), and from continental North America (Talbot et al. 1998) has been sampled by aircraft at altitudes as high as 12 km.

Recent collaborative multi-national, inter-agency experiments such as ACE-1, PEM-Tropics A & B, INDOEX, ACE-Asia, and TRACE-P have included airborne *in-situ* measurements of aerosol optical, chemical, and microphysical properties (Bates et al. 1998; Hoell et al. 1999; Huebert et al. 2003; Jacob et al. 2002; Ramanathan 2001; Raper et al. 2001). These data sets are used to characterize aerosol sources/sinks, to initialize and evaluate chemical transport models (CTMs), to quantify aerosol direct and indirect radiative effects, and to validate satellite retrievals of aerosol optical properties. Use of the airborne observations in these types of investigations requires accurate determination of aerosol properties over a broad range of particle diameters. Aspiration of supermicrometer (D_p >

1.0 μm) particles into high velocity sampling platforms is a significant challenge because of inertial and turbulent losses of the particles within the sampling inlets and carrier tubing (Sheridan and Norton 1998; Wendisch et al. 2004). This difficulty has been known for some time (Huebert et al. 1990) and has stimulated a number of experiments designed to evaluate the magnitude of large particle losses and the efficiency of both active and passive airborne sampling systems (Blomquist et al. 2001; Huebert et al. 2004; Murphy and Schein 1998; Porter et al. 1992). Results from these experiments have shown that discrepancies can exist not only between ground based and airborne sampling systems (Dibb et al. 2002) but also between aircraft flying wingtip-to-wingtip and employing nearly identical instrumentation behind similar inlets (Moore et al. 2004).

NASA sponsored the DC-8 Inlet Characterization Experiment (DICE) in order to characterize the transmission efficiency of aerosol inlets that would potentially be deployed aboard aircraft during the Intercontinental Transport and Chemistry Experiment (INTEX-NA) as well as to investigate measurement discrepancies identified between the NASA DC-8 and NASA P3-B during the TRACE-P mission (Moore et al. 2004). Flights were based out of NASA's Dryden Flight Research Center at Edwards Air Force Base, CA, during May/June 2003. DICE was undertaken to address the following specific questions:

- Does inlet-specific performance compromise our ability to establish submicrometer and supermicrometer aerosol optical properties?
- How do our sampling limitations impact our ability to quantify submicrometer and supermicrometer aerosol surface area and mass?
- What are the size dependent differences of the DC-8 inlet systems?
- How do these differences vary as a function of altitude, air speed, aircraft attitude (pitch, roll, yaw), ambient relative humidity, and aerosol type?
- Whether an actively controlled low turbulence inlet (LTI, (Wilson et al. 2004)) would significantly improve assessment of aerosol surface area or optical properties aboard the NASA DC-8?

DICE instrumentation and flight plans were designed to acquire data over a broad range of aerosol types and sizes within both dry and humid air masses. In this report we focus on quantifying:

- Differences in submicrometer and supermicrometer optical properties measured behind the UH inlet compared to those measured at a ground based station at Edwards Air Force Base (EDW), California and the NOAA/ESRL[i] Coastal Observatory at Trinidad Head (THD), California.
- Differences between supermicrometer aerodynamic size distributions measured behind each of the inlets compared to those measured on the ground at EDW (an environment dominated by mineral dust).
- Inter-inlet differences for supermicrometer scattering and the aerosol size distribution when coarse mode scattering is dominated by mineral dust or sea salt.

[i]Formerly the NOAA Climate Monitoring and Diagnostics Laboratory (CMDL).

Inlets

Ground based measurements of aerosol optical properties and size distributions were conducted on top of the air traffic control tower at Edwards Air Force Base. The EDW ground-station's omni-directional aluminum inlet, modeled after Liu et al. (1983) without a 10 μm impactor, quantitatively sampled aerosols up to 10 μm diameter and has approximately a 50% sampling efficiency for 15 μm diameter particles in wind speeds at least up to 7 m s^{-1} (Maring et al. 2000). Ground based measurements of marine aerosol optical properties were conducted at the NOAA/ESRL Observatory at Trinidad Head, California. The 50% sampling efficiency is calculated at 8 μm aerodynamic diameter for light to moderate winds (J. Ogren, personal communication).

University of Hawai'i Shrouded Solid Diffuser Inlet

The University of Hawai'i shrouded solid diffuser inlet was designed by Dr. Antony Clarke and used aboard the NASA P3-B during PEM-Tropics A & B and TRACE-P (Clarke et al. 2004; Moore et al. 2003). It was designed for a nominal volumetric flow rate of 100 lpm and features a shrouded constant-area flow region around the inlet; a 4.5-degree diffuser half-angle and, a 3.8 cm (inner diameter) tube with the largest possible radius of curvature to complete a 45 degree bend to bring the air into the fuselage (Table 1 and Figure 1a). Spacer rings (not shown) at the base of the shroud can be inserted to adjust the shroud position and the cross sectional area between the shroud and the tip face. The inlet tip has a minimum diameter of 5.13 mm with a curved leading edge (0.25 mm radius) to reduce flow separation at the tip. During the DICE experiment the inlet was tilted down six degrees from horizontal to facilitate iso-axial sampling. This offset is based on the modeled flow field for the DC-8 fuselage during normal flight speeds and pitch. During DICE the bracing window plate was also fitted with a wind vane in order to qualitatively evaluate the degree of iso-axial sampling. The system has since been upgraded to electronically evaluate iso-axial sampling with 0.25° precision.

Previously, Huebert et al. (2004) have shown that the University of Hawai'i shrouded solid diffuser inlet (UH-SDI in Huebert et al.) performs far better than the community aerosol inlet (CAI) deployed aboard the NCAR C-130 during INDOEX and the ACE-1 experiments (Blomquist et al., 2001). Figure 12 of Huebert et al. (2004) indicates that the ratios of silicate mass passed by the UH inlet (UH-SDI) compared to the *uncorrected* low turbulence inlet (LTI) was within the values expected for LTI

TABLE 1
Summary of DICE inlets characteristics

Inlet	UH	LaRC pre-mod.	LaRC post-mod.	UNH
Tip ID (mm)	5.13	3.35	5.13	7.77
Diff 1/2 angle (deg)	4.5	7.0	7.0	8.0
Tube ID (cm)	3.8	2.2	2.2	5.1
Tube Bend (deg)	45	70	70	30
Shroud Type	Constant flow	Constant diam.	Constant diam.	Constant diam.
Q @ 120 m/s (vlpm)	150	63	150	360
Q @ 220 m/s (vlpm)	270	120	270	660
Tip Re @ 120 m/s	42000	27000	42000	65000
Tip Re @ 220 m/s	22000	15000	22000	35000
Tube Re @ 120 m/s	5600	4200	9700	10000
Tube Re @ 220 m/s	3000	2200	5200	5500
$D_{ae,50\%}$ (μm) @ 120 m/s	5.0		3.6	4.1
$D_{ae,50\%}$ (μm) @ 220 m/s	3.2		2.2	2.6
$D_{g,50\%}$ (μm) $\rho = 2.6$ g/cm^3 @ 120 m/s	3.1		2.2	2.5
$D_{g,50\%}$ (μm) $\rho = 2.6$ g/cm^3 @ 220 m/s	2.0		1.4	1.6

enhancement effects for up to 10 μm. Calculating LTI enhancements for marine aerosol is more difficult due to the hygroscopic nature of sea salt under ambient conditions (i.e., RH $>$ 40%). Thus the ratio of marine aerosol mass measured by the UH solid diffuser compared to the LTI is more difficult to assess. Nevertheless the Huebert et al. result indicates a 50% passing efficiency (w.r.t. *uncorrected* LTI) of dry diameters in the 3–4 μm range. During PELTI no direct intercomparison with ground or ship-based measurements of aerosol optical properties or size distributions was possible. As a result, it was impossible to independently measure the optical properties and size distribution of the ambient aerosol from a surface platform in order to ascertain the absolute passing efficiencies of the airborne active and passive inlet systems.

NASA Langley Research Center Small Shrouded Diffuser Inlet

The LaRC inlet (Figure 1b) is a scaled-down version of the University of New Hampshire shrouded diffuser inlet (Figure 1c) described below. It has an inlet tip diameter of 3.35 mm, a diffuser half-angle of 7° and expands to a transport tube diameter of 25.4 mm (Table 1). The inlet mates to a standard, window-mounted gas-sampling probe with an inner diameter of 22 mm and a 20 cm radius of curvature to complete a 70° bend into the aircraft cabin. The inner surface of the gas probe was expanded at a 20° angle to a 25.4 mm diameter to seamlessly mate with the aerosol inlet diffuser. Inlet flows were monitored with a 0–100 lpm mass flow meter located just upstream of the system's venturi exhaust port. Excess flow was adjusted manually to maintain the tip flow velocity within 10% of the aircraft true air speed. At a typical DC-8 air speed of 180 m s^{-1} under isokinetic sampling, the inlet system reduces the flow velocity by a factor of 57 and provides 95 liters per minute of volumetric flow. Constructed for use measuring aerosol scattering and absorption properties aboard the DC-8 aircraft during the TRACE-P field deployment (Jordan et al. 2003a), the inlet was subsequently used aboard that aircraft to support aerosol optical property and soot mass measurements during SOLVE-II. During DICE it was mounted in the same window position, but on the opposite side of the aircraft as the UH inlet.

University of New Hampshire Shrouded Diffuser Inlets

The University of New Hampshire (UNH) shrouded diffusers were based on preliminary design of Dr. Robert Talbot used aboard the NASA Electra during the ABLE campaign. Dr. Talbot and engineers at NASA Ames redesigned the inlets prior to their deployment aboard the faster NASA DC-8 during PEM West A & B, PEM Tropics A & B, SUCCESS, SONEX, and TRACE-P (Dibb et al. 1996, 1997, 1998, 1999a, 2000, 1999b, 2003; Jordan et al. 2003b; Talbot et al. 1998). The probe includes two identical inlets, each employing curved leading edge diffusers centered in a shroud that extends 20 cm forward of the nozzle (Figure 1c). The diffusers expand from the initial diameter of 7.77 mm at 8° to meet the 5 cm outer diameter seamless stainless steel inlet which bends 30° with a radius of curvature of 43 cm to penetrate the aircraft window plate (Table 1). Sampling isokinetically at an air speed of 180 m s^{-1}, the inlets supply 526 lpm of volumetric flow that is manually adjusted to be isokinetic within 10% along each level flight leg. On each deployment one inlet was used to quantify soluble ions in the aerosol phase while the second was used to quantify the radionuclide tracers ^{7}Be and ^{210}Pb.

Instrumentation

Comparisons of inter-inlet and aircraft versus ground-based measurements of the aerosol size distribution were undertaken using Thermo Systems Inc. (TSI) model 3321 aerodynamic

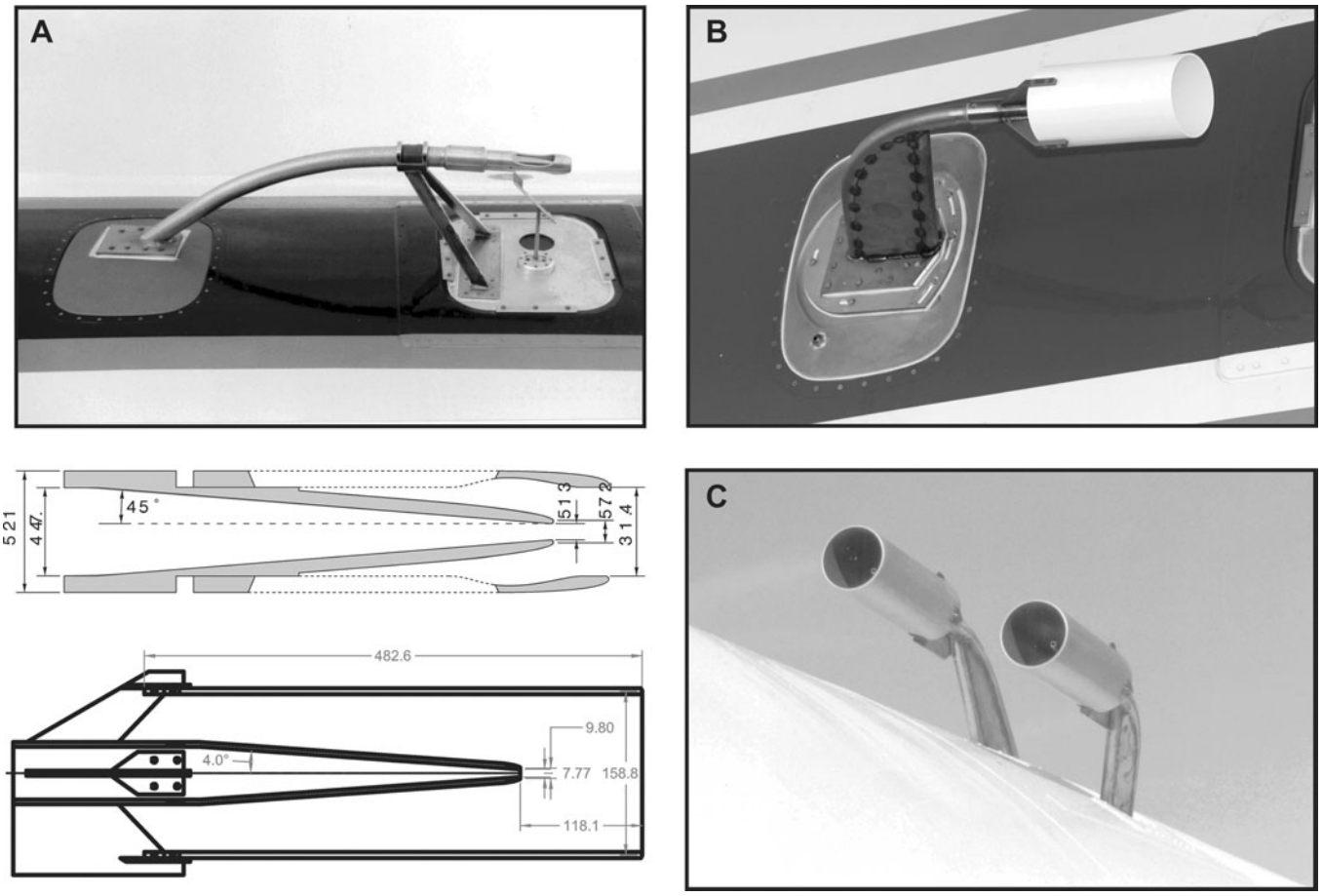

FIG. 1. The University of Hawai'i (A), NASA Langlcy Research Center (B) and University of New Hampshire (C) solid diffuscr inlets mounted on the NASA DC-8. A schematic of the UH (top schematic) and UNH (bottom schematic) inlet tips and shrouds (dimensions in mm) are also included. Below the University of Hawaii's round observation port is a small wind-vane used qualitatively during DICE to evaluate the degree of iso-axial sampling due to airspeed, pitch, roll and yaw. The wind-vane system has since been upgraded and now records deviations from iso-axial sampling conditions electronically with ∼0.25° precision.

particle sizing (APS) instruments. These instruments classify aerosol in the 0.523–20.0 μm aerodynamic size range and include the upgraded firmware components reducing the so-called "ghost particles" problem identified in the TSI model 3320 APS units. Periodically the APS units were removed from the aircraft in order to conduct flow calibration and instrument comparisons. APS sample flows were calibrated to 1.000 ± 0.025 lpm while sheath flows were calibrated to 4.000 ± 0.010 lpm (i.e. ± 2.5% nominal) using a NIST[ii] traceable Gilian Gilibrator-2 bubble flow meter calibration system.

Sample flow was delivered from each inlet through identically machined flow-splitting manifolds mounted on each instrument rack and then through identical lengths of 1.27 cm (inner diameter) carbon-impregnated conductive silicone tubing. APS sample temperature and relative humidity were measured using Vaisala 50Y RH & T sensors.[iii] The sensor's protective sheaths were removed to increase time response and were nested in Swagelock tees upstream of the APS inlets such that they did not impede flow into the APS units.

Each instrument rack measured aerosol scattering at a single wavelength ($\lambda = 540$ nm) using Radiance Research Model M903 nephelometers (RRNephs) plumbed with identical lengths of 0.95 cm ID carbon-impregnated conductive silicone tubing. Flow rates were controlled at 4.00 vlpm using Alicat Scientific volumetric flow controllers. RRNeph temperature and relative humidity were also measured using Vaisala RH & T sensors. The sensors were embedded directly in the RRNeph sample outlet without their protective sheath.

Total and submicrometer aerosol scattering ($\sigma_{sp,tot}$, $\sigma_{sp,sub}$) was measured behind the University of Hawai'i solid diffuser inlet using two TSI model 3563 3-λ integrating nephelometers (Anderson et al. 1996; Heintzenberg and Charlson 1996). The submicrometer TSI nephelometer employed a 1-μm aerodynamic impactor dynamically controlled at 30 vlpm using an Alicat Scientific volumetric flow controller. Surface sites at

[ii]National Institute of Standards and Technology (USA).
[iii]Manufacturer stated accuracy ±2% RH and ±0.1°C.

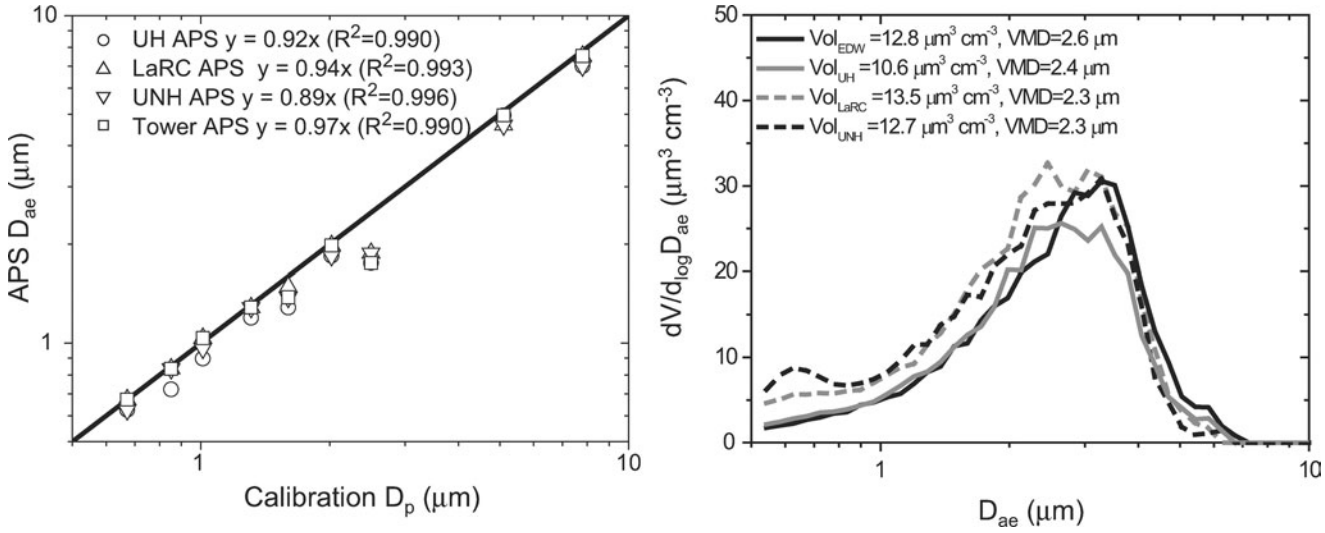

FIG. 2. Each of the APS units accurately sized polystyrene latex spheres (PSL) and borosilicate glass beads (glass) during calibration excercises (left). The glass bead results (Dp > 2.5 μm) have been adjusted for a particle density of 2.5 g cm^{-3}. Sixteen-minute intercomparison of all four APS instruments prior to flight operations during the DICE campaign (right). Although integral volumes are within 15% we observe diverging counting behavior below 1.0 μm and therefore elected to report statistics for $D_{ae} > 0.84$ μm.

Edwards Air Force Base and the observatory at Trinidad Head also measured aerosol scattering using TSI three-wavelength integrating nephelometers. Similar nephelometer measurements at Trinidad head included five minutes of operation in "total" mode followed by five minutes with a 1-μm aerodynamic impactor in "submicrometer" mode. Except where noted, the nephelometer data have *not* been corrected for truncation effects according to (Anderson and Ogren 1998) since we are interested in comparing inlet performance and not in determining precise estimates of the radiative properties of the coarse mode aerosols.

Instrument Calibration

Initially and prior to flights 4 and 7 and after flight 8 (last DICE flight) the RRNephs were calibrated using filtered air and room temperature CO_2 as the zero and span gases. Slight deviations from the target zero and span were noted during the calibration prior to flight 7. As a result the RRNeph data from flights 5 and 6 have been adjusted according to:

$$\mathrm{UH}\_\sigma_{sp} = 0.0 \cdot 10^{-6} + \frac{1}{0.96} \cdot \mathrm{UH}\_\sigma_{sp} \quad [1]$$

$$\mathrm{LaRC}\_\sigma_{sp} = 1.1 \cdot 10^{-6} + \frac{1}{0.95} \cdot \mathrm{LaRC}\_\sigma_{sp} \quad [2]$$

$$\mathrm{UNH}\_\sigma_{sp} = -0.5 \cdot 10^{-6} + \frac{1}{1.0} \cdot \mathrm{UNH}\_\sigma_{sp} \quad [3]$$

The DC-8 TSI nephelometers were calibrated prior to flights 4 and 6 and following flight 8 using filtered air and CO_2. In-flight Raleigh zeros and checks of system zero using a low pressure-drop HEPA filter were periodically performed. The TSI nephelometer on the air traffic control tower was calibrated prior to its installation and after the field campaign. The TSI nephelometer at Trinidad Head (NOAA/ESRL) is periodically calibrated using the same methods (J. Ogren, personal communication).

The sum of nephelometer uncertainties due to noise and calibration for the 550 nm wavelength ($\delta\sigma_{sp}$) is estimated at 0.4 Mm^{-1} for a 25-second measurement based on a 300-second calibration and 300-second zeroing period (Anderson et al. 1996). This error is propagated in quadrature with the standard deviation of the mean during the 25-second time periods included in the statistical analysis in the Appendix. For longer integration times at the ground stations (all longer than 3 minutes) nephelometer uncertainties are assumed to be negligible.

Prior to flight operations, extensive calibrations and intercomparisons were made on the APS units installed aboard the DC-8 and the EDW tower using polystyrene latex spheres (PSL) and borosilicate glass beads (glass) of geometric diameters 0.672, 0.852 1.01, 1.31, 1.60, and 2.5, 5.1, and 7.8 μm (Figure 2, left). The instruments were also operated for several hours at a location adjacent to the flight line where they sampled ambient air including local pollution and mineral dust. This comparison (Figure 2, right) revealed concentration differences and differing values of the volumetric median diameters (VMD) that were largest for submicrometer sizes. Consequently, except where noted, APS size distributions and integral properties are reported for $D_{ae} \geq 0.84$ μm ($D_g = 0.49$ μm for, $\rho = 2.6$ g cm^{-3}).

During flights 5 and 6 the APS installed on the University of New Hampshire instrument rack (UNH APS) appeared to be under-sizing the aerosol size distribution. Post-processing of APS integral volumes indicated that when performance tests included switching between inlets (i.e., the UH inlet was sampled by the UNH instrumentation and vice versa) obvious differences occurred that were not matched by corresponding differences

in the RRNeph scattering data. Prior to flight 7, laboratory tests conducted using calibration spheres indicated that the UNH APS was under-sizing by about 2 channels (channel offset ranged from 1–4 with no size dependence) and the UH APS was under-sizing by about 1 channel (channel offset ranged from 0–3 with no size dependence) whereas the LaRC APS size registration was accurate. Inlet tips were cleaned and sample and sheath flows for each of the APS units were checked and recalibrated to eliminate these sizing offsets. Because of these considerations the APS data from flights 5 and 6 were corrected for this sizing offset (i.e., UH and UNH $dN/d_{log}D_{ae}$ data have been reallocated to larger size classes by 1 and 2 bins, respectively). This effectively eliminated these instrument differences, which were not a result of differing inlet performance.

Experimental Design

Comparison of airborne to ground or ship-based *in-situ* measurements of aerosols and trace gases is notoriously difficult due to instrument and calibration differences, flight altitude and aircraft performance issues as well as the shallow and sometimes layered structure of the planetary boundary layer. Less obvious and seldom discussed is the necessary consideration of integration times. Aircraft flying at 50–220 m s^{-1} sample a larger airmass volume in a shorter time period than either ground or ship-based instrumentation. As an example, a one-minute sample obtained aboard an aircraft traveling at 100 m s^{-1} corresponds to a 20-minute sample obtained on the ground assuming a wind speed of 5 m s^{-1}. Not only wind speed but wind direction must also be considered for representative comparisons and in order to avoid contamination of either platform. In order to compare the airborne and surface-based measurements during DICE we assume there is no temporal evolution of the aerosols during the required sampling intervals. As we will see, in some cases this assumption is not valid.

Our approach is to first compare aerosol light scattering from the TSI 3-λ nephelometer measured behind the University of Hawai'i solid diffuser inlet to similar ground-based measurements during horizontal flybys and vertical profiles. Flybys were conducted in both a dry dust-influenced environment (Mojave Desert, CA) and the wet sea-salt influenced environment (Pacific Ocean near Trinidad Head, CA).

We then compare the relative performance of the three different inlets. These comparisons include measurements of aerosol light scattering from the Radiance Research nephelometers and APS aerodynamic size distributions. The airborne vs. ground-based APS size distribution allow us to determine the 50% passing efficiencies of the inlets for mineral dust particles. No concurrent ground-based measurements of the aerosol size distribution were made in the marine airmasses near THD. This precludes a determination of the 50% passing efficiency of supermicrometer sea salt particles.

During the DICE field campaign an APS and a 3-λ nephelometer were installed on top of the air traffic control tower (∼50 m) at Edwards Air Force Base. The aircraft would typically approach the runway complex from the NE then descend to less than 100 m over the flat, dry surface of the Rogers Lake playa. The aircraft then passed ∼100 m south of the EDW tower before climbing to 300 meters approximately five kilometers down range to avoid low hills. Digital videos of three DC-8 flybys can be found at: http://www-gte.larc.nasa.gov/dice/DICE_Video.htm.

The EDW flybys were designed to compare airborne and ground based measurements in a region where the coarse mode aerosol is dominated by mineral dust. The extremely dry conditions at the NASA Dryden Flight Research Center (DFRC) site within the Mojave Desert also eliminated concerns associated with changing aerosol size in response to relative humidity. Thermal convection coupled with persistent winds over the dry lakebeds typically mixed dust over a relatively deep (>1 km) planetary boundary layer. Although the airborne and tower observations were usually well correlated, high winds and/or mobile emission sources (aircraft) at times produced spatially patchy aerosol loadings (dust devils, exhaust plumes) that lead to significant differences between samples collected from the two platforms, even when flight paths were performed at the same altitude and within 100 m of the EDW tower.

On the Pacific coast near Eureka California, the National Oceanic and Atmospheric Administration (NOAA) Earth System Research Laboratory (ESRL) operates the Trinidad Head Observatory (THD) (http://www.cmdl.noaa.gov/obop/). This site was selected for sampling marine aerosol due to our ability to descend near the site over the Arcata airport on approach. The proximity of the small airport allowed the DC-8 to complete multiple passes of THD at altitudes as low as 100 meters. The goal of flybys at THD was to compare optical properties in a region with coarse mode aerosol dominated by sea salt.

THD is often overcast due to orographic lifting of maritime air. Sea-surface temperatures can be colder than the air temperature. This leads to high boundary layer humidity resulting in significant growth of soluble aerosol (e.g., sea-salt) and coastal fog. Wind speed and direction can change by tens of degrees between the coast and further offshore. Measurement differences due to boundary layer gradients between the aircraft flight altitude and the ground station were assumed small as the observatory resides on a seaside cliff (elev. 107 masl) and the DC-8 aircraft was able to fly at ∼100 m for most passes. More uncertain is the prevailing wind speed and directions near the coast compared to those found offshore when the DC-8 attempted to sample "upwind" of the surface site. Where relevant these issues are discussed in more detail in the case studies that follow.

Finally, despite careful calibrations and intercomparisons of instruments on the aircraft and at the ground stations, absolute differences in instrument performance can occur. Since this potential problem was identified early in the field campaign we devised alternate flow paths whereby either the LaRC or the UNH instrument rack could periodically draw sample air from the UH inlet and vice versa. The required crossover sample lines

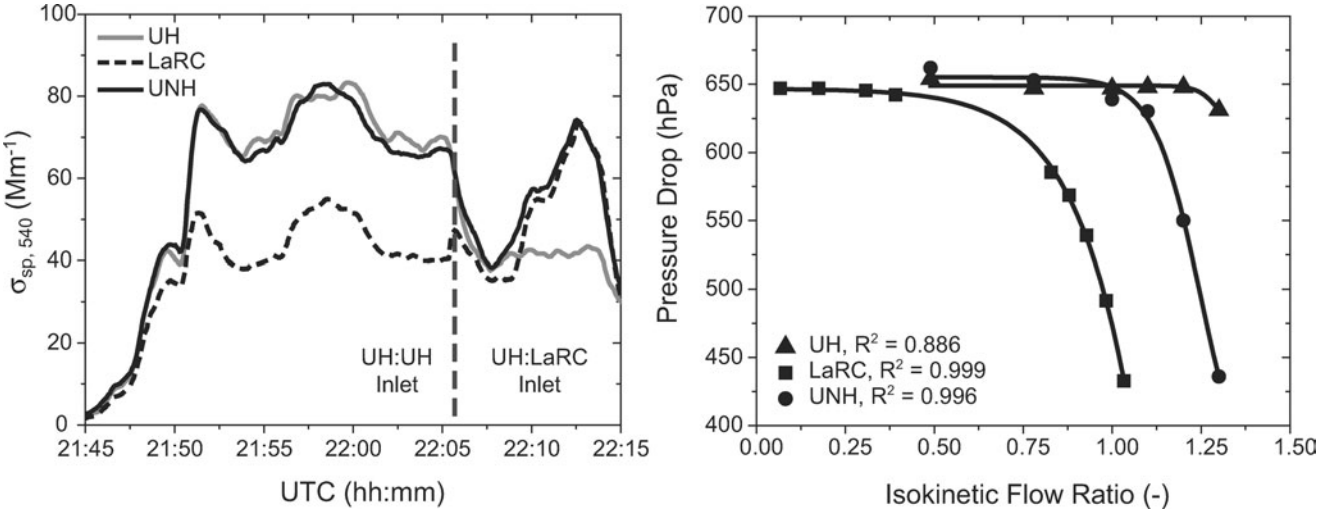

FIG. 3. Total scattering measured by the RRNephs behind each inlet during flight 3 (left). Swapping sample air between UH and LaRC inlets at 22:06 indicated that the LaRC inlet was not sampling coarse mode aerosols effectively. Tests of the pressure drop through the inlet as a function of the isokinetic flow ratio showed the problem was partly due to choked flow in the LaRC inlet (right).

are longer, increasing large particle losses due to gravitational settling. However, losses in each line should be nearly identical as the crossover tubing was identical in length. This "inlet swapping" was often employed during alternating passes of EDW and THD allowing us to check for instrument zero and span offsets as well as to troubleshoot flow and/or pressure differences. When inlets were "swapped" figures and tables have been annotated to guide the reader.

Preliminary Flight Data and Re-Design of the LaRC Shrouded Diffuser Inlet

Early flight results (Figure 3) from a series of low passes over THD indicated that the LaRC shrouded diffuser inlet was much less efficient at transmitting large particles than either the UNH or the UH inlets. Exchanging sample inlets produced a significant decrease in the UH RRNeph scattering coefficient and a corresponding increase in the LaRC RRNeph scattering coefficient. This indicated that the large discrepancy between measurement systems is primarily related to inlet and not instrument performance. Comparison of APS size distributions recorded behind the inlets confirmed that the LaRC inlet suffered much higher relative losses in the supermicrometer size range (not shown).

Ideally, downstream of the diffuser we expect to see a slight increase in inlet pressure with respect to ambient conditions associated with the decrease in flow velocity (i.e., ram pressure). Tests of the pressure drop inside the inlets relative to ambient pressure and as a function of isokinetic flow rate were conducted on DICE flight 4. These tests revealed that the LaRC inlet pressure began to decrease significantly at about 60% of isokinetic flow and dropped dramatically as isokinetic flow was approached. The inlet was experiencing "choked flow," i.e., for tip velocities lower than isokinetic conditions flow rates could not be increased without significantly decreasing the pressure within the inlet.

To better understand and potentially correct the poor performance of the LaRC inlet, its shroud was removed prior to flight 5; this had little obvious effect on the sampling efficiency. After flight 5 the inlet tip diameter was increased from 3.18 mm to 5.13 mm to simulate the UH inlet tip. For flights 6, 7, and 8 the LaRC inlet pressure was similar to the other inlets and the relative performance (with shroud) improved. Even so, this analysis confirmed that the discrepancies noted in Moore et al. (2004) were real and that the inlet itself requires redesign. For the purpose of this manuscript we will show data only from flights 6, 7, and 8, as these are most representative of the inter-inlet performance.

Comparisons of Airborne and Ground-Based Measurements of Aerosol Scattering

Aerosol Scattering Over the Mojave Desert of California

During flight 5 (RF05) the DC-8 completed two passes by the EDW tower while all of the inlets ran isokinetically. Although the TSI nephelometer on the EDW tower was operating at a very low flow rate (∼2 lpm) that resulted in losses of large particles, its measurements allowed us to compare the tower and DC-8 values of $\sigma_{sp,sub}$. Using a 12.5-minute integration time corresponding to 25 seconds of flight data, the mean for the tower and aircraft measurements of $\sigma_{sp,sub}$ are within 2% for the two passes. We refer to this as the "instantaneous" comparison between the aircraft and the tower. Appendix Table A contains a detailed statistical analysis of the mean and standard deviations of each pass.

Mean values and one standard deviation for $\sigma_{sp,tot}$ and $\sigma_{sp,sub}$ measured during flight 5 vertical profiles at EDW are binned into

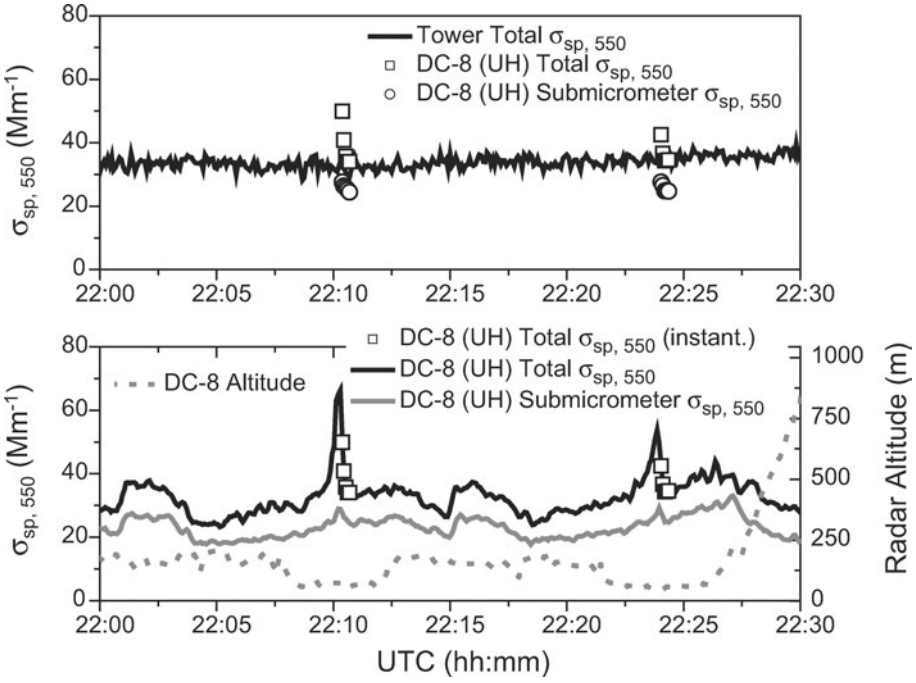

FIG. 4. Instantaneous comparison of total and submicrometer aerosol scattering (550 nm) measured aboard the DC-8 compared to the values measured at the EDW tower for DICE Flight 06 on June 11, 2003 (top). Large discrepancies between the DC-8 and the EDW tower are the result of small-scale enhancements in coarse scattering near the tower probably due to aircraft activity over the runway complex. This is shown in the time series (bottom) of DC-8 scattering during the flybys. Note that the central points for each instantaneous 5-data-point pass are those closest to the tower and do not show the scattering enhancement, i.e., the tower was just upwind of the affected airmass.

100-meter increments for comparison with $\sigma_{sp,sub}$ measured at the tower. The aircraft measurement of $\sigma_{sp,sub}$ in the lowest 100 meters (40.5 ± 3.6 Mm^{-1}) is in excellent agreement with the tower measurements of $\sigma_{sp,sub}$ (42.8 ± 2.4 Mm^{-1}). Note that the aircraft data are all points collected in the lowest 100 meters (50 to 150 meters) including the inbound descent profile, two race-track passes of the tower, and the outbound ascent. We refer to these near tower operations as the aircraft "dwell time." The tower data is the average during the aircraft dwell time. Since the profile data cannot be compared to an equivalent volume of sample air at the tower, this comparison is not suitable for statistical analysis in Appendix Table C.

During DICE research flight 6 (RF06), the DC-8 completed two passes by EDW tower with all inlets sampling isokinetically. The tower nephelometer now operated at 30 lpm flow rate allowing us to compare $\sigma_{sp,tot}$ between the tower and the DC-8 (Figure 4, top). Tower integration time is 3.75 minutes for an equivalent aircraft sample period of 25 seconds (DC-8 TAS = 125 m s^{-1}, EDW WS = 14 m s^{-1}).

Results from the first pass indicate only three of the five 5-second data points are comparable to the ground measurements (Figure 4, top). For the second pass, four of five points show excellent agreement. However, the time-series of scattering from the DC-8 over the EDW runway (Figure 4, bottom) shows that there were two large deviations of $\sigma_{sp,tot}$ with smaller deviations in $\sigma_{sp,sub}$ compared to the remainder of the data collected at low altitude. Winds were from 214° at 14 m s^{-1} and would have a tendency to blow along the main runway, oriented along ~250°, and located south of both the aircraft taxi ramp and the tower. The approach was made from the NE and the time series shows that it is the downwind (w.r.t. EDW tower) portions of the approach that are most influenced by what appears to be aircraft activity over the airfield. By eliminating the influence of this localized aerosol plume (the first two data points of pass #1 and the first data point of pass #2) variances converged and percent differences between the tower and the DC-8 are reduced to at most 4% (compare "RF06 pass #1 & #2" to "RF06 pass #1 & #2—corrected" in Appendix Table A). This exercise illustrates the care needed to identify small-scale atmospheric structures that can influence inter-platform comparisons of aerosol optical properties.

Comparisons of $\sigma_{sp,tot}$ show excellent agreement during vertical profiles on RF06 despite the fact that the standard deviation in the aircraft measurements was three times that measured at the tower. The larger standard deviation is due to the small scale but relatively high aerosol scattering downwind from the runway. If we eliminate sixteen consecutive data points from each pass (1.3 minutes of data from 6.5 minutes of data during each pass) which corresponds to the large deviations from the background observed in the time series data, the difference in aircraft mean of $\sigma_{sp,tot}$ is reduced from 7.5% to only 1.5%. Again, the comparison of tower samples and the aircraft samples during

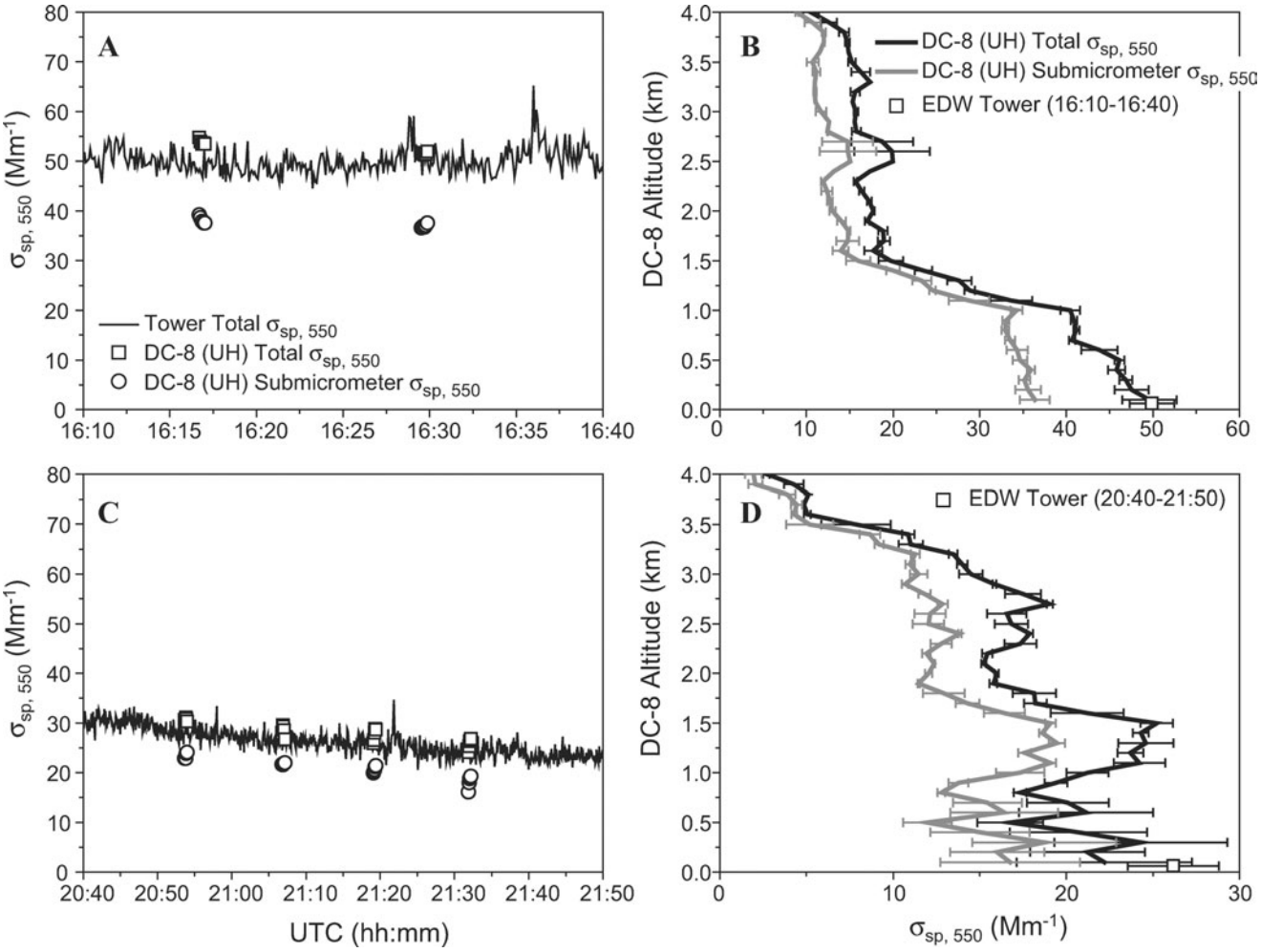

FIG. 5. Instantaneous values (left) and vertical profiles (right) of aerosol scattering measured aboard the DC-8 compared to the values measured at the EDW tower during the morning (Panels A & B) and afternoon flybys (Panels C & D) for DICE flight 8 on June 17, 2003.

the vertical profile are only indicative as they do not sample identical airmass volumes.

During DICE research flight 8 (RF08) six isokinetic passes of the EDW tower were made, two in the morning and four in the afternoon (Figure 5). Mean and standard deviations for the ground station measurement (25-minute integration time) and the 5-point aircraft values for the two flybys agreed to within 5% (Appendix Table A). For the afternoon flybys the winds remained light and variable at the tower and the integration time is the same as the morning. Panel C of Figure 5 shows that over the 130-minute comparison period the $\sigma_{sp,tot}$ decreased approximately 20% from 30 Mm^{-1} to 24 Mm^{-1} at the EDW tower. Results from the instantaneous comparisons are excellent (less than 3% difference) and they capture not only the magnitude but also the decreasing trend in aerosol scattering. Note that the trend is not the same for total and submicrometer scattering. The airborne measurements indicate an increase in coarse mode fraction of scattering from 24% to 29% (±2%) between the first and the last afternoon passes.

Vertical profiles of $\sigma_{sp,tot}$ and $\sigma_{sp,sub}$ over EDW for the morning and the afternoon flybys are plotted in panels B & D of Figure 5. The tower and aircraft mean $\sigma_{sp,tot}$ are identical for the morning profile (<1% difference). In the afternoon this difference is 15%. The standard deviation of $\sigma_{sp,tot}$ for the afternoon profile is comparable to morning, however the magnitude of $\sigma_{sp,tot}$ is approximately half the values measured earlier in the day. Thus the coefficients of variation in the lowest 100 m of the airmass are also higher than measured locally by the DC-8 earlier in the day (6% vs. 22%). The apparent increase in heterogeneity is probably linked to the light and variable winds as well as localized convection above the desert/dry lakebeds up and down-range from the air traffic control tower in the late afternoon. Recall that the mean of the aircraft data are for all points below 150 meters whereas the tower's mean is that of the aircraft dwell time (1 hour 10 minutes for the afternoon) so the means being compared are not samples of equivalent airmass volume. Agreement between the aircraft and the tower for the morning profile data is excellent and probably linked to relatively homogeneous conditions. However, as

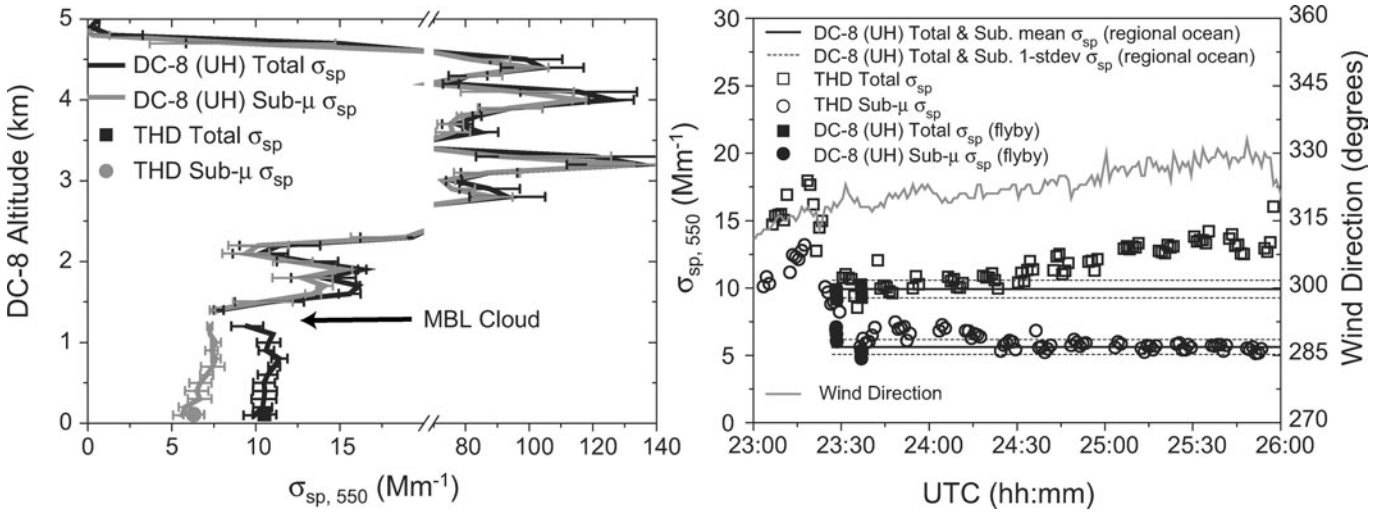

FIG. 6. Vertical profile (left) of aerosol scattering ($\lambda = 550$ nm) measured over the Arcata airport near the NOAA/CMDL Trinidad Head Observatory by the DC-8 aircraft compared to the values measured at Trinidad Head between 23:30 and 24:40 (UTC) for DICE Flight 07 on June 13, 2003. Time series (right) of total and submicrometer aerosol scattering measured; at THD (open symbols), during the DC-8 flybys (solid symbols), and during DC-8 upwind flight legs (black lines). Nephelometer relative humidities were 29% at THD compared to 27% aboard the DC-8. Wind direction (grey lines) became more along-shore during the intercomparison.

patchiness increases, inter-platform comparisons must consider spatial and temporal collocation of the measurement and include appropriate integration times based on platform velocities, wind speed, and direction.

Aerosol Scattering in the MBL at Trinidad Head (THD), California

On DICE research flight 7 (RF07) the DC-8 completed a vertical descent over the Arcata airport, two passes by THD, followed by an upwind leg over the ocean. Figure 6 shows the vertical structure of $\sigma_{sp,tot}$ and $\sigma_{sp,sub}$ during the DC-8's descent into Arcata as well as the average $\sigma_{sp,tot}$ and $\sigma_{sp,sub}$ measured at THD during the aircraft dwell time.

The difference between ground and aircraft $\sigma_{sp,tot}$ are –3.2% and +7.7% for passes #1 and #2 while the differences in $\sigma_{sp,sub}$ are –16% and <1% (Appendix Table B). The large difference between the DC-8 and the THD measurements of submicrometer scattering during the first flyby is in part due to changing airmass character as measured by the THD station just prior to the aircraft comparison at 23:30 UTC (Figure 6, right).

After the THD flyby the DC-8 continued NW of the surface site at an altitude of 300 meters in order to characterize aerosols within the maritime air blowing onshore at THD. At an aircraft speed of 120 m s^{-1} traveling NW for 6.5 minutes the corresponding integration time for the THD tower at an average wind speed of 6 m s^{-1} is 130 minutes. Variability of aerosol scattering over the open ocean was low and Figure 6 (right) shows the mean and standard deviation for the scattering measured during the upwind aircraft leg ("regional ocean"). $\sigma_{sp,sub}$ at THD prior to 24:42 UTC was, in general, elevated with respect to the values measured upwind by the DC-8 instrumentation. When the THD scattering values are averaged until the shift in wind speed and direction at 26:06 UTC the difference between the DC-8 and THD is reduced to ~10%.

Total scattering, $\sigma_{sp,tot}$, measured aboard the DC-8 is within 6% of the THD values for the first hour of the integration time (23:30–24:36 UTC). After 24:36 total scattering begins to diverge from the values measured aboard the aircraft. Since submicrometer scattering remains the same this indicates temporal evolution of the supermicrometer aerosol over the 130-minute integration time. This divergence is likely the result of shifting wind direction (315° to 330°). Due to the orientation of the coastline, coastal aerosols including those generated by nearshore breaking waves possibly influenced the airmass sampled at THD. While flying over the open ocean the DC-8 samples would not include coarse mode aerosols generated in the nearshore environment. Despite the possibility of these influences the aircraft and ground-station data agree within 30%.

On June 17, 2003 (DICE flight 8) the DC-8 completed another vertical descent over Arcata airport followed by four racetrack passes by THD. Winds were light and variable from the South at the surface. Under these conditions, the aircraft's 25-second sampling time integrates an equivalent of 25 minutes surface data.

The profile values of $\sigma_{sp,tot}$ and $\sigma_{sp,sub}$ were 4.8% and 28% higher than THD but were conducted over the Arcata airport and therefore poorly collocated spatially. For the lowest 100 m of the DC-8 profile $\sigma_{sp,coa}$ accounts ~40% ((24.8–15.2)/24.8 Mm^{-1}) of $\sigma_{sp,tot}$ indicating that the airmass contains significant supermicrometer sea salt aerosols. Using the average over the 1-hour integration of σ_{sp} at THD the coarse mode fraction of scattering estimate is ~50% ((23.7–11.9)/23.7 Mm^{-1}).

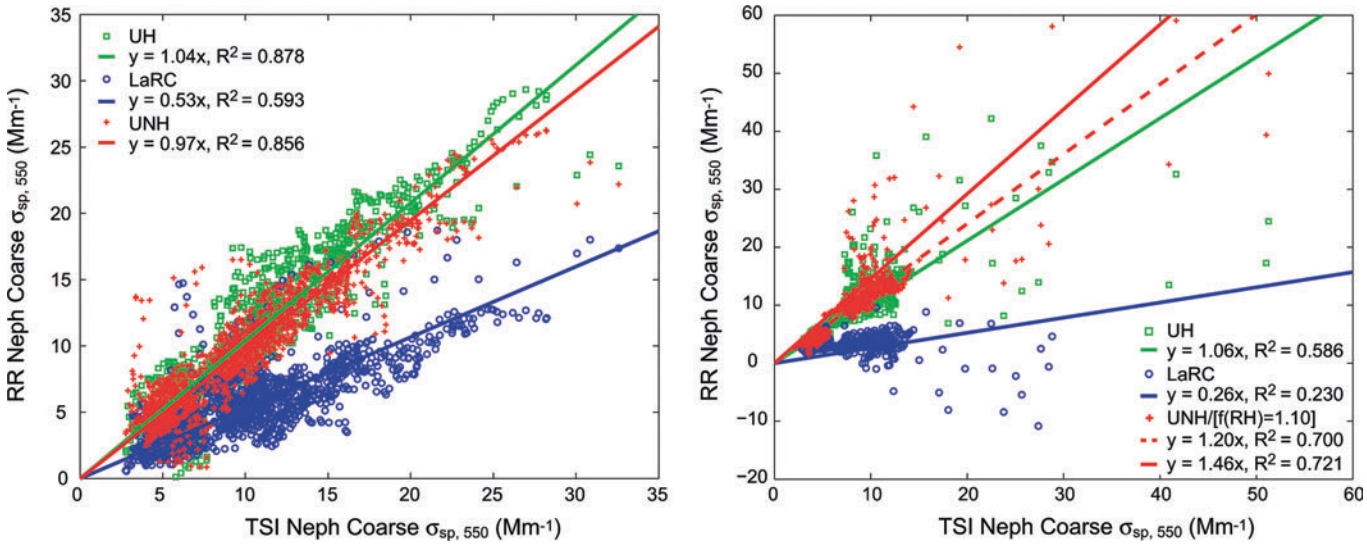

FIG. 7. (a) RR nephelometer coarse ($D_{ae} > 1.0\ \mu m$) scattering vs. TS1 nephelometer coarse scattering ($\lambda = 550$ nm) during DICE flights 5, 6, and 8 when aerosol volume is dominated by mineral dust. There is excellent agreement between the Hawai'i and New Hampshire inlets. However, by subtracting the submicrometer scattering from the total scattering we see that the LaRC inlet captures only ~50% of the coarse mode scattering (b) RR nephelometer coarse ($D_{ae} > 1.0\ \mu m$) scattering vs. TS1 nephelometer coarse scattering ($\lambda = 550$ nm) during DICE flights 7 and 8 when aerosol volume is dominated by sea salt. UNH RRNeph total scattering data was divided by f(RH) = 1.10 before subtracting the subniicrometer component of scattering. Solid lines indicate best fits of the uncorrected data. The dashed line indicates the best fit for the UNH data after correction and suggests that the UNH inlet captures ~13% more light scattering than the UH inlet for coarse aerosols dominated by sea salt.

Differences between the DC-8 and THD range from –16% to +30% for the total and submicron aerosol scattering. However, the systematically lower UH total scattering and systematically higher UH submicrometer scattering results in a UH supermicrometer estimate only 55% the THD value (Appendix Table B and C). Relative humidity was comparable between the instrument systems and variability of $\sigma_{sp,tot}$ measured aboard both the DC-8 and at the ground station are both low. This suggests the regional airmass was homogeneous in the horizontal. The cause of the large supermicrometer discrepancy is not readily apparent but is probably related to difficulties associated with airborne sampling of marine aerosols at high (95%) ambient relative humidity.

Inter-Inlet Comparisons of Aerosol Scattering Using Radiance Research Nephelometers

A detailed examination of the scattering coefficients measured behind each inlet allows us to evaluate their relative performance. For this analysis, our standard is the previously discussed $\sigma_{sp,tot}$ and $\sigma_{sp,sub}$ measurements provided by the two TSI model 3563 nephelometers that drew sample from the UH inlet. Also, by subtracting the TSI $\sigma_{sp,sub}$ (free of inlet losses as indicated by pass #1 & #2 from RF05) from $\sigma_{sp,tot}$ measured by the Radiance Research (RRNeph) and the TSI nephelometer ($\sigma_{sp,tot}$), we can evaluate the inter-inlet performance with regard to coarse mode scattering ($\sigma_{sp,coa}$) in these environments.

Two corrections were made to the RRNeph data to facilitate these comparisons. First, the total RRNeph $\sigma_{sp,540}$ were increased by the empirical relationship:

$$\sigma^{RR}_{sp,540} = \frac{\sigma^{RR}_{sp,540}}{0.94 - 0.25 \cdot (1 - FF_{scat})} \quad [4]$$

where

$$FF_{scat} = \frac{\sigma^{TSI}_{sp,540}(Dae < 1\ \mu m)}{\sigma^{TSI}_{sp,540}(total)} \quad [5]$$

This relation was derived by Anderson et al. (2003) and normalizes Radiance Research nephelometer performance to TSI nephelometer performance based upon the relative coarse mode fraction of scattering (1 minus fine-mode fraction of scattering, FF_{scat}). Second, time lags due to sample line lengths, sample-volume flushing times, and instrument averaging were computed and a 7-point smoothing Gaussian filter was applied to the TSI nephelometer data. Co-registration of peaks in supermicrometer scattering as well as the shape of the signal decay is well represented by this averaging scheme.

Figure 7a shows RRNeph $\sigma_{sp,coa}$ versus TSI $\sigma_{sp,coa}$ for each 5-second data point collected during research flights 5, 6, and 8 where the aerosol volume was dominated by mineral dust. Intercepts were forced through zero because when left unconstrained the intercepts were $\pm 1\ Mm^{-1}$, which is at the level of RRNeph instrument precision. Linear regression for the RRNeph $\sigma_{sp,tot}$ versus TSI $\sigma_{sp,tot}$ are not shown, but produced slopes of 1.01 ($R^2 = 0.977$), 0.87 (0.950), and 1.00 (0.977) for the UH, LaRC, and UNH inlets, respectively.

The correlation coefficients for RRNeph $\sigma_{sp,coa}$ are somewhat lower compared to the regressions based on RRNeph $\sigma_{sp,tot}$. For both the UH and UNH inlets slopes remain within 10% of each other and within 5% of unity (recall that TSI $\sigma_{sp,tot}$ and $\sigma_{sp,sub}$ are measured behind the UH inlet exclusively). Based on this level of agreement we conclude that the UH and UNH inlets are performing comparably in the desert environment whereas the LaRC inlet only samples ~55% of the supermicrometer aerosols responsible for coarse mode scattering. We also surmise that the Anderson et al. (2003) correction to the RRNeph scattering values is an effective means of normalizing Radiance Research nephelometer scattering to that derived from TSI nephelometers.

In order to determine the relative performance of the inlets while sampling sea salt aerosols in the marine environment, an analysis similar to that described above was performed for scattering coefficients measured within the marine boundary layer during flights 7 and 8. Results are shown in Figure 7b. Again, intercepts were forced through zero ($\pm$ 1 Mm^{-1} when left unconstrained). The slope near unity (1.06) for the UH inlet confirms relative performance is consistent with the mean Anderson et al. correction. The higher slope (1.46) for $\sigma_{sp,coa}$ measured behind the University New Hampshire inlet suggests the inlet samples marine aerosol with a greater efficiency than the University of Hawai'i inlet. However, the slightly lower temperature and higher average RH within the UNH RRNeph, 37% ($\pm$2% for Vaisala RH sensors) compared to 23% within both the UH and LaRC RRNephs (29% and 26% within the TSI "total" and "submicrometer" nephelometers behind UH inlet), coupled with the hygroscopic nature of sea salt aerosols may account for part if not all of this difference even though these RH values are "low."

For example, although Carrico et al. (2003) measured crystallization relative humidities (CRH) of 41% $\pm$ 1% for marine aerosols in the Pacific between Hawaii and Japan during ACE-Asia, they also observed f(RH) values of 1.05–1.10 for relative humidity changes between 38% and 40%, when marine/pollution aerosols crystallized and transitioned from the upper to the lower branch of their hysteresis loop. This is consistent with the observations of Tang et al. (1997) that, unlike pure NaCl particles, sea salt particles do not return to their initial weight immediately after drying. The author's state, "There is always some residual water remaining in sea salt particles." It is also possible that the aerosol matrix sampled in the MBL during the DICE flights may include sulfates and organic aerosols, which do not deliquesce in the same manner as sea salt.

To illustrate the potential for scattering enhancements due to residually bound water, we divide the total UNH RRNeph scattering values (at 37% RH) by f(RH) = 1.10 *before* subtracting $\sigma_{sp,sub}$ measured by the TSI nephelometer (26% RH). The dashed line in Figure 7b represents the best fit for the UNH f(RH) "corrected" data. The UNH inlet appears to transmit more particles responsible for ~14% more light scattering compared to the UH inlet. For comparison the slope of RRNeph:TSINeph $\sigma_{sp,tot}$ is 1.03 ($R^2 = 0.888$), 0.70 (0.831), and 1.20 (0.911) for the UH, LaRC and UNH inlet without corrections and 1.09 (0.911) for the UNH inlet with the humidity correction. Consequently, the difference between UH and UNH performance could be largely a result of differing instrument relative humidity.

Comparisons of Aerodynamic Aerosol Size Distributions

A number of factors make comparison of supermicrometer aerosol mass or volume-based size distributions difficult. Volume median diameters (VMD) measured by some optical particle counting methods (like the FSSP-300) have been reported as 2–3 times greater than aerodynamic counting methods (such as the APS) or inversion methods (e.g., size distributions derived from AERONET data) (Reid et al. 2006; Reid et al. 2003a). Since the mission was conducted in regimes where large particles are present in low concentrations, poor sampling statistics in the supermicrometer size range could potentially impact our inter-platform comparisons of aerosol volume. This is particularly problematic when comparing data from sampling platforms (or instruments), such as aircraft and towers that employ different techniques, sample flow rates, and integration times.

During the DICE experiment coefficients of variation of supermicrometer aerodynamic aerosol volume for the ground-based APS measurements were on the order of 25–50% over 25-minute time intervals. After pooling the same data into five, 5-minute intervals coefficients of variations were on the order of 10–20%. In our analysis we have been careful to appropriately scale (through ratios of tower wind speed to aircraft speed) and then pool the tower size distributions before comparing them to the five 5-second APS size distributions measured aboard the DC-8. This is an important consideration as it ensures that the volume of the boundary layer air sampled by the instrument platforms is comparable and that variability of the aerosol properties is adequately accounted for.

The omni-directional aluminum inlet on top of the EDW air-traffic control tower has a 50% sampling efficiency for 15 μm diameter particles in wind speeds at least up to 7 m s^{-1} (Maring et al. 2000). In our analysis we implicitly assume that there were no aerosol particle losses in this inlet. Appendix Table D compares airborne and ground based supermicrometer aerodynamic aerosol volume using two-tailed Student's *t*-tests for each pass of the EDW tower during flights 6 and 8. Appendix E compares aerosol bulk chemistry measurements between the DC-8 and the tower as well as between mass derived from the APS instruments. Appendix Table F compares supermicrometer light scattering calculated from the size distributions for the two high-dust cases and four low-dust cases during DICE flight 8.

Theoretical Versus Observed Passing Efficiency of Mineral Dust

Flow regime, either laminar or turbulent, is governed by the ratio of the inertial force of the fluid (in this case air) to the force of friction of the air moving over the aerosol particles' surface (Baron and Willeke, 2001). This dimensionless quantity, the Reynolds Number (Re), as a function of altitude for each inlet at the tip of the diffuser as well as in the carrier tubing

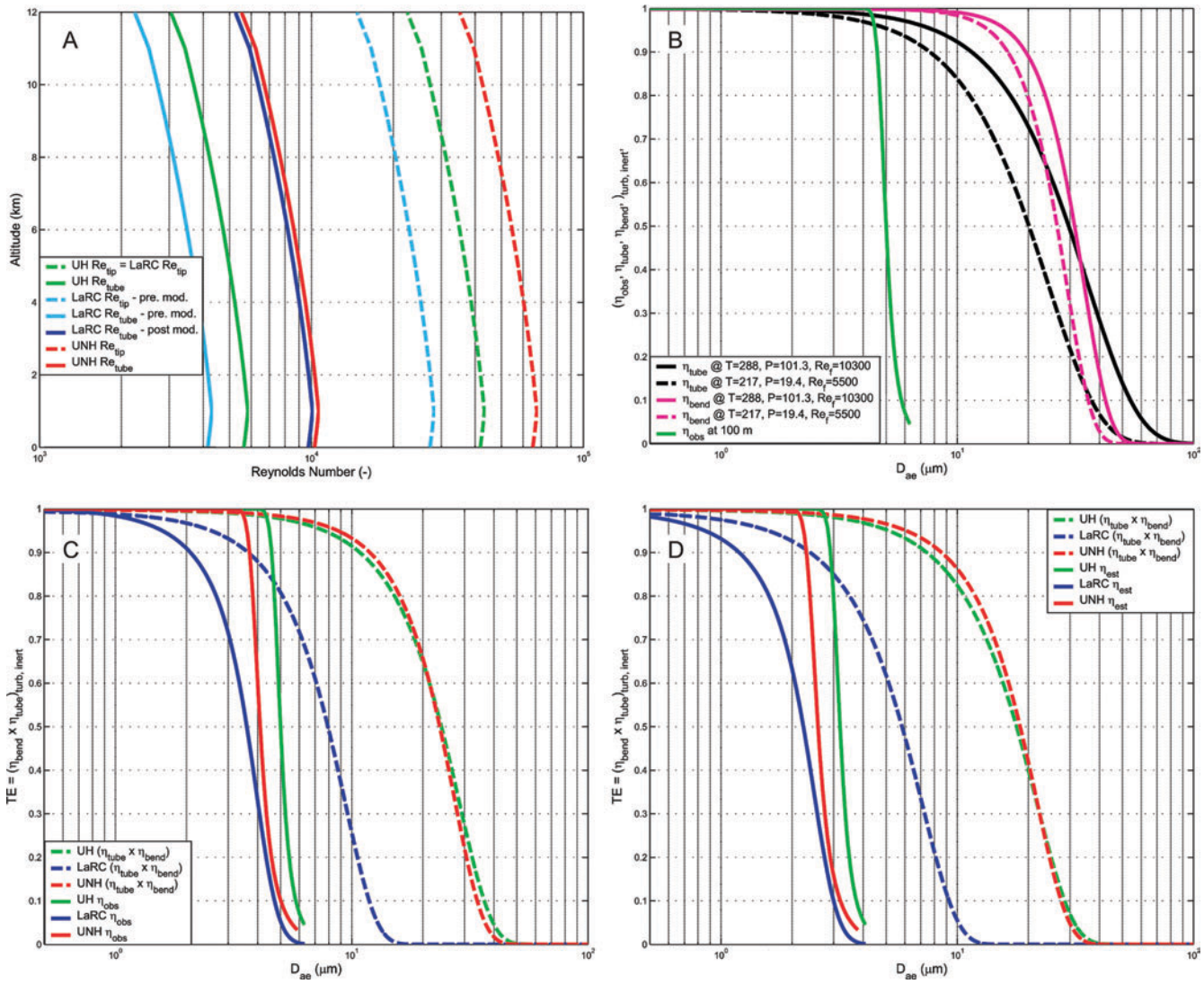

FIG. 8. Reynolds numbers for the inlet tips and carrier tubing (A). Theoretical turbulent inertial losses for the UH inlet inside the carrier tubing and for a 45° bend (computed at the surface and at 12 km) compared to the observed losses at the surface (B). Observed compared to theoretical losses for all three inlets at the surface (C). Theoretical losses for all three inlets at 12 km compared to an esimate based on the observations at the surface (D). Truncation of the observed transmission efficiency curves is due to poor counting statistics at a threshold uncertainty of 50%.

behind the diffuser are shown in Figure 8a and summarized for each inlet in the lower portion of Table 1. Calculations are based on a standard atmospheric profile for temperature and pressure (Rogers and Yau 1989) and assume a linearly increasing true airspeed of 120 m s^{-1} at the surface, 220 m s^{-1} at 12 km. Re for the LaRC inlet tip after modification is equal to that of the UH inlet. The pre-modification LaRC diffuser has the lowest Re values due to the small cross section of the tip, 8.8 cm^2. But as we saw in Figure 3 this resulted in choked flow and reduced pressure within the LaRC sampling system. The UH and UNH inlets have tip areas of 20.7 and 50.3 cm^2 but do not experience choked flow while sampling isokinetically (Figure 3, right).

Turbulent inertial losses for each inlet system were modeled using equations 8–61 and 8–68 of Baron and Willeke (2001). Tubing losses ($\eta_{\text{tube,turbinert}}$) are modeled over a 2 m length for each inlet. Losses in the tubing bend ($\eta_{\text{bend,turbinert}}$) are modeled as 45° bend for the UH inlet, 70° bend for the LaRC inlet and a 30° bend for the UNH inlet. Losses in the inlet diffuser and at the flow splitting manifolds aft of the aircraft inlets are not considered here.

Figure 8b show the theoretical turbulent inertial losses for each component of the UH inlet at both the surface and 12 km. Figure 9a compares the airborne vs. EDW aerodynamic size distributions during RF08 Pass #1 a case where aircraft aerosol volumes are all statistically ($\alpha = 0.05$) lower than the ground based measurements (Appendix Table D). This case, along with RF08 pass #2, are the only cases during DICE where particles with aerodynamic diameters larger than ~5 μm were measured by the EDW tower APS.

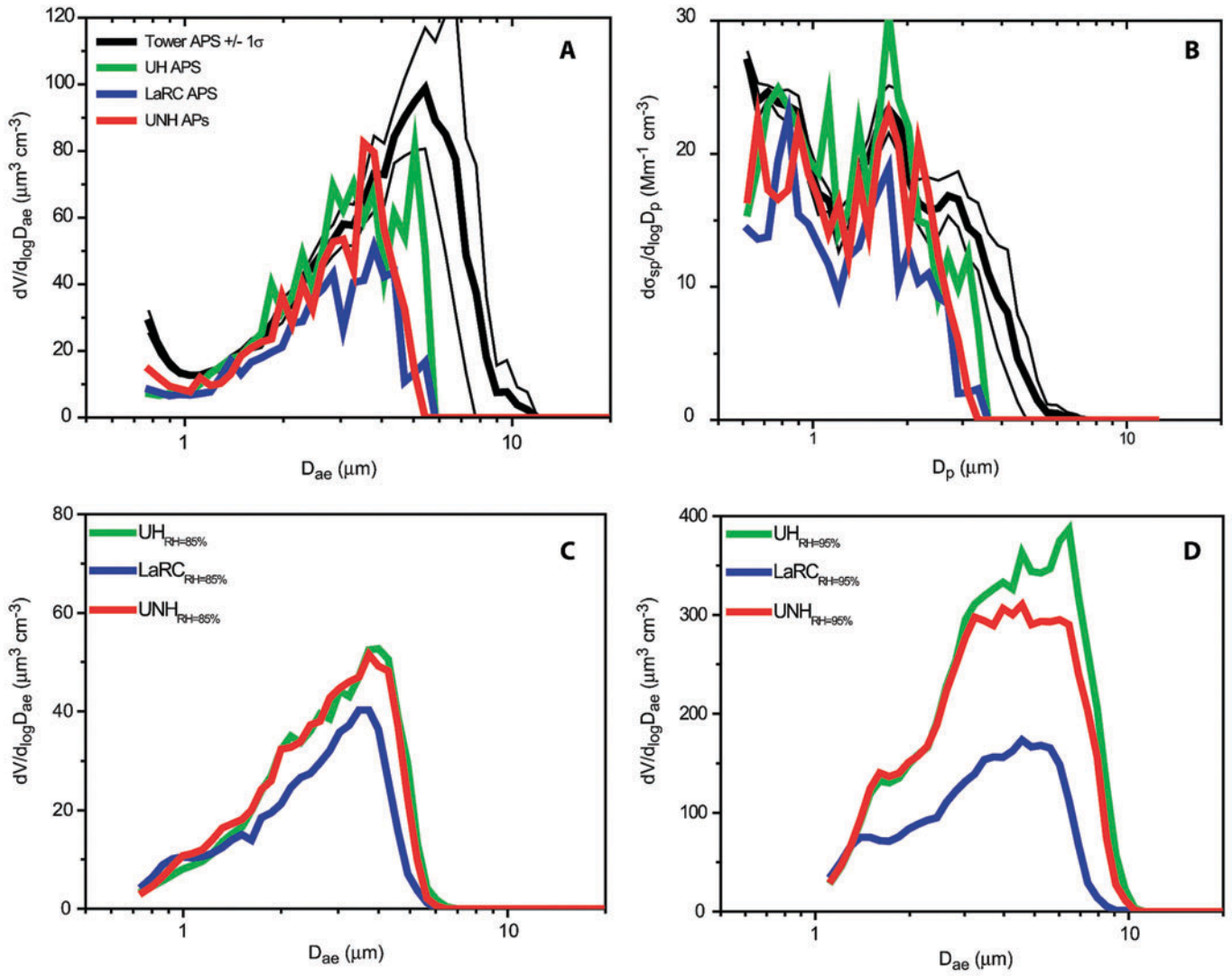

FIG. 9. Mean of five 5-second aerodynamic size distributions for mineral dust aerosols measured at 60 m over the Rogers Dry Lake compared to 25-minutes of 5-second data at the EDW tower (A). Corresponding scattering size distribution (B) to the aerodynamic distribution in A. Mass scattering efficiency decreases with increasing particle geometric diameter. Therefore the UH and UNH inlets recorded 88% and 73% of the aerosol light scattering despite only recording 67% and 52% of the supermicrometer aerosol volume. Ambient humidity aerodynamic size distributions for sea salt aerosols measured for 25 minutes (C) and 35 minutes (D) at 300 m over the Pacific Ocean near Trinidad Head California. The APS distributions have been adjusted using hygroscopic growth factors of 1.86 and 2.89 to reflect ambient vs. instrument (dry) relative humidity. In the marine environment the UH and UNH inlets perform nearly identically while the instrumentation behind the LaRC inlet recorded only 76% and 45% of the volume recorded behind the UH inlet. Largest losses were associated with the highest ambient relative humidity.

The observed UH inlet efficiency curve (steep truncated curve in Figure 8b) is calculated by pooling the data from all the EDW passes where inlet swapping had not occurred and where significant ($\alpha = 0.05$) differences were identified between the ground-based and the airborne aerodynamic size distributions. Truncation occurs at a threshold instrument count of four particles over the integration time corresponding to an estimate with 50% uncertainty. The relatively sharp cut is probably due to the observation that aerosol measured at the EDW tower rarely contained supermicrometer particles larger than $\sim$5 μm.

All three-inlet efficiency curves are shown in figure 8c along with the combined, theoretically derived, losses in the inlet tubing and through the tubing bend. For the University of Hawai'i and University of New Hampshire inlets $D_{ae,50}$ is 5.0 μm and 4.1 μm and the inlets show a relatively steep cut. The modified LaRC inlet $D_{ae,50}$ value is 3.6 μm but the shape of the curve indicates that a $\sim$10% loss of aerosol volume is occurring at an aerodynamic diameter of 2.0 μm. The aerodynamic efficiency curves measured at the surface were converted to the corresponding efficiency curves at 12 km (T = 217K, P = 19.4 hpa, μ-1.56 $\times$ 10^{-5} Pa·s) by matching the Stokes' number of the particles and ignoring the effects of fluid compression at high Mach number. These are compared to the combined theoretical losses for 12 km in Figure 8d. The $D_{ae,50}$ at 12 km correspond to diameters of 3.2, 2.2, and 2.6 μm for the UH, LaRC, and UNH inlets.

Converting the aerodynamic equivalent diameter (i.e., $\rho = 1.0$) to geometric equivalent diameter using a particle density of 2.6 g cm^{-3}, the 50% passing efficiency for the UH inlet is 3.1 μm at the surface and 2.0 μm at 12 km. For the LaRC inlet the values of $D_{g,2.6}$ are 2.2 μm at the surface and 1.4 μm at 12 km. For UNH, $D_{g,2.6}$ is 2.5 μm at the surface and 1.6 μm at 12 km. Incorporating a dynamic shape factor, χ, would tend to increase the geometric diameter that can be effectively sampled but has not been applied.

Inter-Inlet Comparisons in the Marine Environment Near Trinidad Head, California

No measurements of the aerosol size distributions were made at the THD ground station thus inter-inlet performance when sampling sea salt is a relative comparison only. Dry aerodynamic size distributions of marine aerosols measured near Trinidad Head California were first corrected for near-particle non-Stokesian flow in the APS 3321 using a dry sea salt density of 2.2 g cm^{-3}. The UH and UNH instruments recorded dry (RH $<$ 40%) aerosol aerodynamic volumes of 8.7 μm^3 cm^{-3} for flight 7 and volumes of 23 and 20 μm^3 cm^{-3}, respectively, during flight 8. Ambient atmospheric relative humidity for RF07 and RF08 were 85% and 95% with ~2% uncertainty. APS aerodynamic particle sizes were converted to equivalent geometric sizes using a dry sea salt density of 2.2 g cm^{-3}. To scale geometric particle sizes at instrument relative humidity (dry) to ambient relative humidity, we use humidity growth factors, GF, of 2.15 (δ_{GF} = 2.08–2.22) and 2.89 (δ_{GF} = 2.62–3.42) for sea salt at a relative humidity of 85% (±2%) and 95% (±2%) (Howell et al. 2006). Ambient geometric diameters were then scaled to ambient aerodynamic diameters using hydrated particle densities of 1.15 g cm^{-3} ($\delta\rho_{85\%}$ = 1.16–1.14) and 1.06 g cm^{-3} ($\delta\rho_{95\%}$ = 1.08–1.04). Thus supermicrometer aerosol aerodynamic volume at ambient RH was 30 μm^3 cm^{-3} behind both the UH and the UNH inlets during RF07 and 175 and 155 μm^3 cm^{-3} behind the UH and UNH inlets during RF08 (Figure 9c, 9d).

Figure 9c and 9d illustrate that the UH and the UNH inlets have nearly identical performance characteristics (within instrument precision) and outperform the modified LaRC inlet. The truncation of the aerodynamic distributions measured in the marine environment at 85% RH (Figure 9c) appear to support the steep $D_{ae,50}$ cut established at 5.0 and 4.1 μm for the UH and UNH inlets. The LaRC inlet only records 76% the volume recorded behind the other two inlets consistent with its much broader efficiency curve. However, the UH and UNH distributions adjusted to 95% relative humidity are truncated at diameters in excess of 7.0 μm. Although the efficiency of their transmission is not known, and humidification growth factors are uncertain at high RH, UH, and UNH cut sizes of 5.0 and 4.1 μm appear to be conservative estimates.

Comparison of Ground-Based and Airborne Bulk Aerosol Chemistry Measurements

Filter-based bulk aerosol chemistry measurements were collected at the EDW tower as well as aboard the DC-8 behind the second UNH inlet. Filters are then extracted with methanol and deionized water and analyzed by ion chromatography (Dibb et al. 2002).

A comparison of filter-based chemistry measurements at the EDW tower and the DC-8 was not possible for RF06 due to small-scale differences in the aerosol field (see Figure 4). On RF07 and RF08 chemistry measurements were obtained over the ocean during operations near the Trinidad Coastal Site. Although no chemistry measurements were made at THD the DC-8 bulk chemistry results can be compared to APS derived mass behind the UH and UNH inlets.

APS aerodynamic diameters were corrected to volume equivalent diameters using a dry seasalt density of 2.2 g cm^{-3} without a shape-factor correction. The filter measurements during RF07 were consistent with nearly pure seasalt in the coarse mode, with Ca:Mg = 0.18 and Ca:Na = 0.024 (seawater ratios are 0.19 and 0.020). Nearly identical masses from the chemical measurements and calculated from the APS using a seasalt density of 2.2 g cm^{-3} suggest that there was no significant mass other than seasalt and that the sample inlet and plumbing to the filters and APS had essentially the same particle transmission efficiency (Appendix E). In contrast, the filter data from RF08 showed elevated calcium ratios (Ca:Mg = 0.51 and Ca:Na = 0.057) and the calculated mass from the APS exceeded the sum of the ionic constituents by about 50%, suggesting that dust was present. Assuming that 5% of dust mass is soluble Ca, the excess calcium implies that approximately 20% of the supermicrometer mass was dust. The added mass reduces the filter:APS discrepancy to roughly 35%, within one standard deviation of the APS data. This implies that the seasalt growth factor used in Section 9.2 is an overestimate for ~20% of the particulate mass. The size distributions of the dust and seasalt are presumably different, but we lack size-resolved chemistry, so cannot determine what fraction of the particles should be assigned a lower growth factor.

Aerosol bulk chemistry measurements were also made during both the morning and the afternoon passes of the EDW tower during flight 8. APS aerodynamic diameters were corrected to geometric diameters using a dust density of 2.6 g cm^{-3}. Total dust mass was calculated from the Ca^{2+} concentration assuming calcium is 5% by weight of the total dust mass. The table in Appendix E shows that both the DC-8 bulk chemistry measurements (UNH inlet) and the pooled APS measurements behind the UH and UNH inlets are indistinguishable from the EDW tower chemistry measurements for both the morning and the afternoon RF08 flybys. We do note that our assumption of calcium as 5% by weight of the total dust mass is the best fit to the data and is uncertain.

Inter-Inlet Comparisons of Aerosol Scattering using APS Derived Scattering

Here we use direct measurements of aerosol optical properties ($\sigma_{sp,coa}$) to evaluate the optical properties calculated from the aerodynamically measured size distributions. These calculations are based on realistic assumptions about particle densities, refractive indices, particle morphology, and so on.

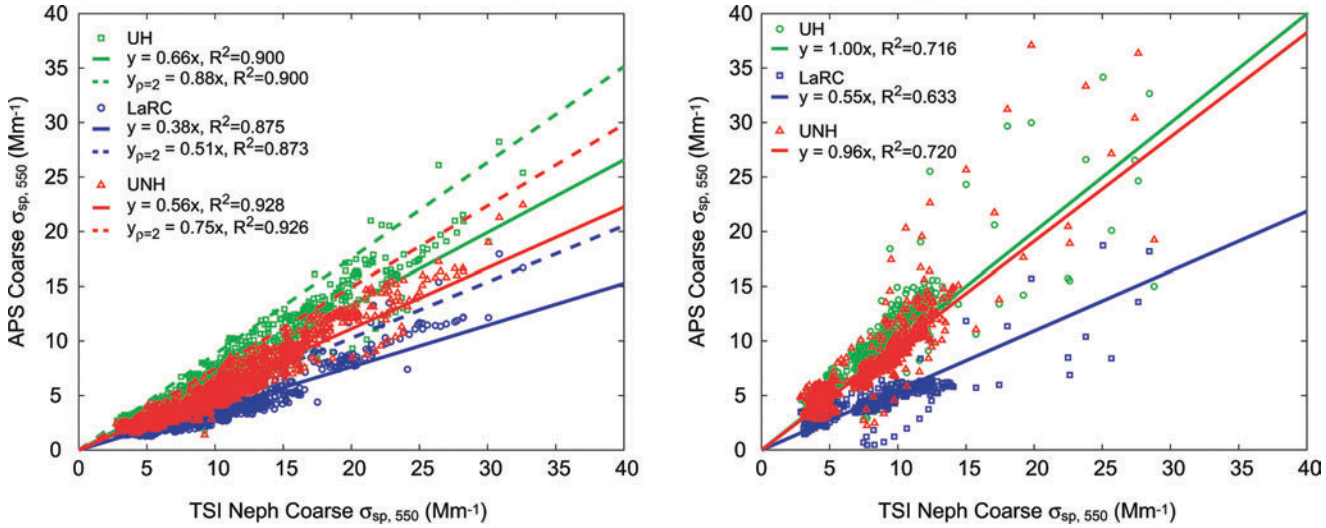

FIG. 10. (a) APS derived scattering (Dp > 1.0 μm, $\rho_{dust} = 2.6$ g cm^{-3}, m = l.53-0.00061) vs. TSI nephelometer coarse scattering ($\lambda = 550$ nm) during DICE flights 5, 6, and 8 when aerosol volume is dominated by mineral dust (solid lines). APS derived scattering for $\rho_{dust} = 2.0$ g cm^{-3} (dashed lines). Correlation coefficients are excellent but suggest that our estimates of particle density and/or refractive index are inadequate. Plot also shows that the UH inlet captures ~18% more scattering particles than the UNH inlet. (b) APS derived scattering ($D_p > 1.0$ μm, $\rho_{seasalt} = 2.2$ g cm^{-3}, m = 1.5688-0.0i) vs. TSINeph coarse scattering (1 = 550 nm) during DICE flights 7 and 8 when aerosol volume is dominated by sea salt. The difference of only 4% between the UH and the UNH APS derived scattering indicates that these two inlets perform identically even when sampling an environment where the aerosol volume is dominated by hygroscopic sea salt aerosols at high (80–95%) relative humidity.

Below we document the parameter values selected for our analysis in an effort to standardize our methods with those of previous publications.

The APS is calibrated with spherical polystyrene (PSL) or borosilicate glass (glass) spheres of known density ($\rho_{PSL} = 1.05$ g cm^{-3}, $\rho_{glass} = 2.52$ g cm^{-3}). Aerodynamic diameters measured by the APS are slightly larger than the true aerodynamic diameters (D_c) due to small-scale turbulence in the flow field induced by the APS on the aerosol particles (near-particle non-Stokesian flow). For 1.0 μm particles this difference is 3.5% for $\rho = 2.6$ g cm^{-3} or, 3.0% for $\rho = 2.2$ g cm^{-3} at T = 298.15K. At 10 μm the difference is 15% and 12%, respectively. Corrected aerodynamic diameters (D_c) were transformed to geometric diameters (D_g) assuming that the particles are spherical and that the densities are the same as used in the Stokes correction (Peters et al. 1993). Light scattering coefficients (550 nm) were calculated using a refractive index of $m_{dust} = 1.53–0.0006i$ for mineral dust (Clarke et al. 2004) and a refractive index for dry sea-salt of $m_{seasalt} = 1.5688–0.0i$ (Tang et al. 1997). Although the real part of the dust refractive index is uncertain and could vary between 1.5 and 1.7, we are most interested in relative agreement between instruments so can ignore this contribution to uncertainty.

Inter-instrument performance of the various APSs generally agreed within about 15% for $D_{ae} \geq 0.84$ μm (Figure 2, right panel). By transforming the APS aerodynamic diameters to geometric diameters and then applying Mie scattering theory we can use the APS size distributions to calculate $\sigma_{sp,coa}$ for $D_{ae} \geq 1.0$ μm. This allows us to compare supermicrometer scattering measured by the TSI nephelometers (UH $\sigma_{sp,coa}$ = UH $\sigma_{sp,tot}$ – UH $\sigma_{sp,sub}$) behind the UH inlet to the supermicrometer scattering size distributions measured behind each inlet. Also, we can then compare supermicrometer scattering size distributions measured behind each inlet to those from the EDW tower distribution. This is a second means of evaluating inter-inlet performance and the inlet's ability to sample optically relevant supermicrometer aerosols.

Figure 10a shows the linear regression between calculated and measured $\sigma_{sp,coa}$ below 300 m over Rogers dry lake during flights 5, 6, and 8. Figure 10b shows the results from the marine aerosols measured during flights 7 and 8. Once again, the regression intercepts were forced through zero because offsets were all less than 2.0 Mm^{-1}.

The mineral dust cases indicate closer agreement between calculated and measured $\sigma_{sp,coa}$ behind the UH inlet compared to either LaRC or UNH. The slope of the regression for the UH APS derived scattering compared to the measured scattering ($\sigma_{sp,tot}$ minus $\sigma_{sp,sub}$) is 0.66. This underestimate could be linked to the assumption that dust particles are spherical. Since dust particles are not spherical but rather angular or fractal in shape they have a higher surface area to mass ratio than spherical particles. This leads to more rapid acceleration in the APS sensing volume and under-sizing. In Figure 10a dashed lines are the results after applying the empirical Reid et al. (2003a) "effective density correction" of 2.0 g cm^{-3} for mineral dusts. Coarse $\sigma_{sp,550}$ is still underestimated by 12% but within measured differences in APS performance (Figure 2), although uncertainties in density, refractive index, and shape factor may also contribute to the difference.

In the marine environment the UH and UNH APS derived supermicrometer scattering is identical within instrument performance differences (Figure 10b). The modified LaRC inlet appears to be losing approximately 50% of the supermicrometer aerosol responsible for light scattering measured behind the UH inlet. This value is consistent with the 45% loss of coarse mode scattering as measured by the Radiance Research nephelometer behind the LaRC inlet.

Comparison of Airborne and Ground-Based Scattering Calculated from APS Size Distributions

Since aerosol scattering efficiency per unit mass is approximately inversely proportional to diameter for supermicrometer sizes, we expect better agreement between values of supermicrometer scattering calculated from the size distributions than agreement between supermicrometer volume (Appendix Table F). In other words, while the small number of large particles lost in the UH and UNH inlets/plumbing account for 67% and 52% of the supermicrometer volume during RF08 Pass #1 (Figure 9a), they should account for a smaller percentage of the supermicrometer scattering.

Figure 9b show the inlets' scattering size distributions for RF08 pass #1 compared to the tower distribution. For RF08 pass #1 supermicrometer scattering behind the UH inlet/plumbing was 88% (14/16 Mm^{-1}) of that measured at the tower. Scattering behind the UNH inlet/plumbing was 75% (12/16 Mm^{-1}) of that calculated from the tower size distributions.

These results demonstrate that closure between airborne and ground-based measurements of supermicrometer aerosol volume can be difficult to achieve, potentially increasing uncertainties associated with supermicrometer measurements of aerosol mass and chemistry. Aerosol optical properties and aerosol surface area are less sensitive to large particle losses resulting in better agreement between airborne and ground-based measurements.

Summary

This study was undertaken in order to quantify both the absolute and relative performance of three passive, solid diffuser type inlets aboard the NASA DC-8 research aircraft. The inlets were designed separately and have been used by the University of Hawai'i, NASA Langley Research Center and the University of New Hampshire to sample aerosols aboard the NASA P3-B and NASA DC-8 during various field campaigns.

When sampling mineral dust aerosols, $\sigma_{sp,tot}$ and $\sigma_{sp,sub}$ measured behind the University of Hawai'i solid diffuser inlet was within 5% of the ground-based measurements in all but one flyby of the EDW ground station. We determined that the outlying case was the result of small-scale enhancements in the local aerosol field due to aircraft activity over the runway complex. In the marine environment, differences between $\sigma_{sp,tot}$ measured behind the UH inlet and those measured at the NOAA/ESRL Trinidad Head Observatory were less than 16%. Differences between DC-8 and THD measurements of $\sigma_{sp,sub}$ were larger than $\sigma_{sp,tot}$ but were still within 30%. No cause could be determined for these relatively large differences although measurements were complicated by high relative humidity (80–95%). Differences in the 50% cut-size of the submicrometer aerodynamic impactors aboard the DC-8 and at THD could also contribute to submicrometer differences especially for coarse sea salt aerosol and if the relative humidity at the impactor plates differs.

Inter-inlet performance was evaluated over the Mojave Desert through an analysis of light scattering as well as supermicrometer aerosol volume and bulk aerosol chemistry. Comparisons of aerosol scattering data recorded over the Mojave Desert indicated that the UH and UNH inlets sampled nearly identically (7% difference) whereas the LaRC inlet failed to pass ~50% of the aerosols responsible for supermicrometer light scattering relative to the UH inlet (see Figure 7a). Evaluations of inlets based on supermicrometer mineral dust volume responsible for light scattering (see Figure 10a) support this finding indicating an 18% difference between the UH and UNH inlets while the LaRC inlet only sampled ~60% of the optically effective aerosol measured by the other two inlets. Filter-based bulk aerosol chemistry measurements (UNH inlet) and aerosol mass calculated from APS aerodynamic size distributions (UH and UNH inlets) were indistinguishable from measurements at the EDW tower assuming a dust density of 2.6 g cm^{-3} (no shape factor correction) and calcium as 5% of the total dust mass.

In the marine environment, the evaluation of inter-inlet performance was complicated due to the effects of differing instrument relative humidity. After attempting to correct for these effects, estimates of coarse scattering differed by only 13% between the UH and UNH inlets whereas the LaRC inlet failed to pass ~75% of the marine aerosol responsible for supermicrometer light scattering (Figure 7b). Scattering calculated from APS measurements of aerosol volume for the UH and UNH inlets were within APS uncertainty (difference of just 4%) whereas the scattering calculated from distributions behind the LaRC inlet were approximately 50% that measured in the other inlets (Figure 10b).

In the appendix a statistical analysis using the Student's *t-test* ($t_{0.05(2),(v1+v2)}$) is used to evaluate the level of agreement between supermicrometer aerosol aerodynamic volume measured at the EDW tower and supermicrometer aerosol aerodynamic volume measured behind each inlet (Table D). Supermicrometer dust volume measured behind the University of Hawai'i inlet and associated tubing were statistically indistinguishable from those measured at the EDW tower for four of the eight flybys. Behind the University of New Hampshire inlet supermicrometer dust volume was also statistically indistinguishable from that measured on the ground in four of the eight flybys. The modified LaRC inlet performed poorest with supermicrometer dust volume recorded behind the inlet indistinguishable from the ground in only one of the eight flybys.

The mean aerodynamic size distributions from the passes completed under normal operating conditions (i.e., no inlet swapping) were pooled and compared to the corresponding, time-integrated distributions measured at the EDW tower. Based

on these size-resolved results the aerodynamic ($\rho = 1.0$) 50% passing efficiency ($D_{ae,50}$) of mineral dust for the inlets is determined to be no less than 5.0 and 4.1 μm for the UH and UNH inlets respectively. However, at the EDW tower few particles were measured beyond $\sim$5 μm in size potentially indicating that these are conservative estimates of the inlet passing efficiencies. This is also consistent with the results of Huebert et al. (2004) for the silicate mass passing efficiency of the UH inlet. The 50% passing efficiency of the modified LaRC inlet was determined to be 3.6 μm. The broader shape of the observed efficiency curve is consistent with light scattering and aerosol volumes $\sim$50% those recorded at the EDW tower.

A quantitative determination of the 50% passing efficiency of marine aerosols (i.e., supermicrometer sea-salt) was not possible. Ambient aerosol distributions were computed at 95% relative humidity using a sea salt growth factor of 2.89. In this instance the UH and UNH APS instruments recorded ambient diameters as large as 6–8 μm although the efficiency at which these particles were sampled remains unknown.

Supermicrometer aerosol scattering calculated from APS size distributions was compared to supermicrometer scattering calculated from size distributions at the EDW tower. At high dust concentrations, supermicrometer scattering ($\sigma_{sp,coa}$) calculated from the aerosol size distributions differed from the tower values by only 12% (27% while inlets were swapped) behind the UH inlet/plumbing despite only measuring 67% (51% while inlets were swapped) of the aerosol volume. The UNH calculated scattering differed from the tower values by 27% (32% while swapped) while measuring only 52% (46% while inlets were swapped) of the aerosol volume. These results illustrate that while sampling supermicrometer aerosol volume through passive inlets can result in significant losses, this has a much smaller impact on aerosol surface area and aerosol optical properties.

Note that the losses evaluated here are the net effect of both the inlet and transfer tubing to the instruments. Losses were highest when inlet swapping had occurred, i.e., when transfer tubing lengths were longest. Estimates from PELTI suggest that plumbing losses can be on the order of half of all particle losses (Huebert et al. 2004).

CONCLUSIONS

The University of Hawai'i solid diffuser inlet was shown to effectively pass aerosol particles responsible for better than 95% of total light scattering over the Mojave Desert when compared to identical ground-based measurements at the Edwards Air Force Base air traffic control tower (EDW). In the marine environment total and submicrometer light scattering aboard the aircraft was within 10% and 30% of measurements made at the NOAA/ESRL coastal observatory at Trinidad Head, California (THD).

Over an appropriately scaled integration time, the means of supermicrometer aerosol aerodynamic volume measured behind the UH and UNH inlets were statistically indistinguishable from the pooled means measured at the EDW tower in four of the eight aircraft passes ($\alpha = 0.05$). Periodically swapping sample air between instrument racks necessitated longer transfer tubing between the inlets and the instrumentation. This resulted in enhanced large particle losses and poorer agreement between the airborne and ground-based measurements at high dust concentrations. During lower ambient dust concentrations the aerodynamic particle sizer at the EDW tower recorded negligible aerosol volume above 5.0 μm. At these lower dust concentrations inlet swapping had a smaller effect on the results due to the high transmission efficiencies of the UH and the UNH inlets/plumbing in the 3–5 μm aerodynamic size range.

Based on supermicrometer aerodynamic size distributions, the University of Hawai'i, NASA Langley and University of New Hampshire inlets have 50% passing efficiency aerodynamic diameters of 5.0, 3.6, and 4.1 μm, respectively. Thus airborne measurements of aerosol size distributions, their chemical composition, and optical properties can be compared directly to ground or ship-based measurements when dominated by sizes smaller than this.

Using a dust bulk density value of 2.6 g cm^{-3} and ignoring dynamic shape factor considerations (results in a more conservative estimate), the geometric equivalent diameter of these passing efficiencies are, 3.1, 2.2, and 2.5 μm for the inlets. Thus passing efficiencies for the UH and UNH inlets are sufficiently reliable to be comparable with ground-based monitoring standards such as the EPA's[iv] $PM_{2.5}$. However, at higher altitude the ratio of drag forces to inertial forces is reduced. To estimate both the aerodynamic and geometric 50% transmission efficiency diameters at the DC-8 flight ceiling ($\sim$12 km) we assume losses are controlled by phenomenon associated with the particle Stokes number and ignore the effects of fluid compression at high Mach number. The corresponding aerodynamic diameters at 12 km are 3.2, 2.2, and 2.6. Assuming a spherical particle density of 2.6 g cm^{-3} the corresponding geometric diameters are 2.0, 1.4, and 1.6 μm at 12 km. Incorporating a dynamic shape factor, χ, would tend to increase the geometric diameter that can be effectively sampled but has not been applied.

The DC-8 inlet characterization experiment shows that the NASA Langley small shrouded diffuser inlet does not effectively sample supermicrometer aerosols even after modification to the inlet tip diameter. This confirms the findings of Moore et al. (2004). Therefore, we recommend caution when using aerosol optical properties measured behind the earlier unmodified LaRC inlet aboard the DC-8 during TRACE-P and SOLVE II.

Particle surface area and aerosol scattering are generally dominated by sizes smaller than 4 μm. The DICE results show that the University of Hawai'i and University of New Hampshire passive solid diffuser type inlets appear adequate for aerosol sampling objectives aboard the NASA DC-8 during INTEX-NA. However, in environments with more enhanced coarse aerosol such as Asian or Saharan dust storms or the marine boundary

[iv] United States Environmental Protection Agency.

layer under moderate to high winds and high relative humidity, passive inlets will underestimate aerosol volume and, to a lesser extent, light scattering.

While more sophisticated active aerosol inlets are available, their deployment aboard research aircraft involves a larger payload, additional power requirements and post-processing in order to properly account for the size dependent enhancements (Huebert et al., 2004). In contrast the passive solid diffusers' presented here, require no additional space, operators, or power requirements. Past evaluations of active versus passive inlet performance (PELTI) on a lower speed aircraft (NSF/NCAR C-130) showed that the magnitude of corrections needed for particle losses in the solid diffuser inlets at large sizes were comparable to corrections needed for particle enhancements in the Low Turbulence Inlet (LTI). However, direct comparisons to ground based measurements like those presented here were not conducted during PELTI, nor were the comparisons subject to statistical analysis.

REFERENCES

Anderson, T. L., Covert, D. S., Marshall, S. F., Laucks, M. L., Charlson, R. J., Waggoner, A. P., Ogren, J. A., Caldow, R., Holm, R., Qyant, F., Sem, G., Wiedensohler, A., Ahlquist, N. A., and Bates, T. S. (1996). Performance Characteristics of a High-Sensitivity, Three-Wavelength, Total Scatter/Backscatter Nephelometer, *J. Atmos. Oceanic Technol.* 13:967–986.

Anderson, T. L., Masonis, S. J., Covert, D. S., Ahlquist, N. C., Howell, S. G., Clarke, A. D., and McNaughton, C. S. (2003). Variability of Aerosol Optical Properties Derived from In Situ Aircraft Measurements During ACE-Asia. *J. Geophys. Res.* 108 (D23): ACE 15-1-ACE 15–19.

Anderson, T. L., and Ogren, J. A. (1998). Determining Aerosol Radiative Properties using a TSI 3563 Integrating Nephelometer, *Aerosol Sci. Technol.* 29:57–69.

Baron, P. A., and Willeke, K. (2001). *Aerosol Measurement: Principles, techniques, and applications, 2nd ed.* John Wiley and Sons, Inc., New York.

Bates, T. S., Huebert, B. J., Gras, J. L., Griffiths, F. B., and Durkee, P. A. (1998). International Global Atmospheric Chemistry Project's First Aerosol Characterization Experiment: Overview, *J. Geophys. Res.* 103 (D13):16,297–16,318.

Blomquist, B. W., Huebert, B. J., Howell, S. G., Litchy, M. R., Twohy, C. H., Schanot, A., Baumgardner, D., Lafleur, B. G., Seebaugh, W. R., and Laucks, M. L. (2001). An Evaluation of the Community Aerosol Inlet for the NCAR C-130 Research Aircraft, *J. Atmos. Oceanic Technol.* 18(8):1387–1397, doi: 10.1175/1520-0426(2001)018.

Carrico, C. M., Kus, P., Rood, M. J., Quinn, P. K., and Bates, T. S. (2003). Mixtures of Pollution, Dust, Sea Salt, and Volcanic Aerosol during ACE-Asia: Radiative Properties as a Function of Relative Humidity, *J. Geophys. Res.* 108(D23):8650, doi: 10.1029/2003JD003405.

Clarke, A. D., Collins, W. G., Rasch, P. J., Kapustin, C. N., Moore, K., Howell, S., and Fuelberg, H. E. (2001). Dust and Pollution Transport on Global Scales: Aerosol Measurements and Model Predictions, *J. Geophys. Res.* 106 (D23):32555–32569.

Clarke, A. D., Shinozuka, Y., Kapustin, V. N., Howell, S., Huebert, B., Doherty, S., Anderson, T., Covert, D., Anderson, J., Hua, X., Moore, I. K. G., McNaughton, C., Carmichael, G., and Weber, R. (2004). Size Distributions and Mixtures of Dust and Black Carbon Aerosol in Asian outflow: Physiochemistry and Optical Properties, *J. Geophys. Res.* 109(D15):1–20.

Dibb, J. E., Talbot, R. W., Klemm, K. I., Gregory, G. L., Singh, H. B., Bradshaw, J. D., and Sandholm, S. T. (1996). Asian Influence Over the Western Pacific during the Fall Season: Inferences from lead-210, Soluble Ionic Species and Ozone, *J. Geophys. Res.* 101:1779–1792.

Dibb, J. E., Talbot, R. W., Lefer, B. L., Scheuer, E., Gregory, G. L., Browell, E. V., Bradshaw, J. D., Sandholm, S. T., and Singh, H. B. (1997). Distributions of Beryllium-7 and Lead-210 Over the Western Pacific: PEM West B, *J. Geophys. Res.* 102:28,287–28,302.

Dibb, J. E., Talbot, R. W., and Loomis, M. B. (1998). Tropospheric Sulfate Distribution during SUCCESS: Contributions from Jet Exhaust and Surface Sources, *Geophys. Res. Lett.* 25:1375–1378.

Dibb, J. E., Talbot, R. W., Meeker, L. D., Scheuer, E. M., Blake, D. R., Blake, N. J., Gregory, G. L., and Sachse, G. W. (1999a). Constraints on the Age and Dilution of PEM Tropics Biomass Burning Plumes from the Natural Radionuclide Tracer ^{210}Pd, *J. Geophys. Res.* 104:16,233–16241.

Dibb, J. E., Talbot, R. W., Scheuer, E. M., Blake, D. R., Blake, N. J., Gregory, G. L., Sachse, G. W., and Thornton, D. C. (1999b). Aerosol Chemical Composition and Distribution during the Pacific Exploratory Mission, Tropics, *J. Geophys. Res.* 104:5785–5800.

Dibb, J. E., Talbot, R. W., and Scheuer, E. M. (2000). Composition and Distribution of Aerosols Over the North Atlantic during the Subsonic Assessment Ozone and Nitrogen Oxide Experiment (SONEX), *J. Geophys. Res.* 105: 3709–3717.

Dibb, J. E., Talbot, R. W., Scheuer, E. M., Seid, G., Avery, M. A., and Singh, H. B. (2003). Aerosol Chemical Composition in Asian Continental Outflow during the TRACE-P Campaign: Comparison with PEM-West B, *J. Geophys. Res.* 108 (D21), GTE 36-1–GTE 36-13.

Dibb, J. E., Talbot, R. W., Seid, G., Jordan, C., Scheuer, E., Atlas, E., Blake, N. J., and Blake, D. R. (2002). Airborne Sampling of Aerosol Particles: Comparison between Surface Sampling at Christmas Island and P-3 Sampling during PEM-Tropics B, *J. Geophys. Res.* 108 (D2), 8230, doi:10.1029/2001JD000408.

Haywood, J. M., Francis, P. N., Geogdzhayev, I., Mishchenko, M., and Frey, R. (2001). Comparison of Saharan Dust Aerosol Optical Depths Retrieved using Aircraft Mounted Pyranometers and 2-Channel AVHRR Algorithms, *Geophys. Res. Lett.* 28(12):2393–2396.

Heintzenberg, J., and Charlson, R. J. (1996). Design and Applications of the Integrating Nephelometer: A Review, *J. Atmos. Oceanic Technol.* 13:987–1000.

Hoell, J. M., Davis, D. D., Jacob, D. J., Rodgers, M. O., Newell, R. E., Fuelberg, H. E., R.J. McNeal, Raper, J. L., and Bendura, R. J. (1999). Pacific Exploratory Mission in the tropical Pacific: PEM-Tropics A, August-September 1996, *J. Geophys. Res.* 104(D5):5567–5583.

Howell, S. G., Clarke, A. D., Shinozuka, Y., Kapustin, V. N., McNaughton, C. S., Doherty, S., and Anderson, T. (2006). Interactions between Pollution and Dust during ACE-Asia: Size Distributions and Implications for Optical Properties, J. Geophys. Res. *submitted.*

Huebert, B. J., Bates, T. S., Russell, P. B., Shi, G., Kim, Y. J., Kawamura, K., Carmichael, G. R., and Nakajima, T. (2003). An Overview of ACE-Asia: Strategies for Quantifying the Relationships between Asian Aerosols and Their Climatic Impacts, *J. Geophys. Res.*

Huebert, B. J., Howell, S. G., Covert, D. S., Bertram, T., Clarke, A. D., Anderson, J. R., Lafleur, B., G., Seebaugh, W. R., Wilson, J. C., Gesler, D., Blomquist, B. W., and Fox, J. (2004). PELTI: Measuring the Passing Efficiency of an Airborne Low Turbulence Aerosol Inlet, *Aerosol Sci. Technol.* 38, 803–826, doi: 10.1080/027868290500823.

Huebert, B. J., Lee, M. G., and Warren, W. L. (1990). Airborne Aerosol Inlet Passing Efficiency Measurement, *J. Geophys. Res.* 95:16,369–16,381.

Husar, R. B., Tratt, D. M., Schichtel, B. A., Falke, S. R., Li, F., Jaffe, D., Gasso, S., Gill, T., Laulainen, N. S., Lu, F., Reheis, M. C., Chun, Y., Westphal, D., Holben, B. N., Gueymard, C., I. McKendry, Kuring, N., Feldman, G. C., McClain, C., Frouin, R. J., Merrill, J. T., DuBois, D., Vignola, F., Murayama, T., Nickovic, S., Wilson, W. E., Sassen, K., Sugimoto, N., and Malm, W. C. (2001). Asian Dust Events of April 1998, *J. Geophys. Res.* 106(D16):18317–18330.

Jacob, D. J., Crawford, J. H., Kleb, M. M., Connors, V. E., Bendura, R. J., Raper, J. L., Sachse, G. W., Gille, J. C., Emmons, L., and Heald, C. L. (2002). The Transport and Chemical Evolution over the Pacific (TRACE-P) Aircraft Mission: Design, Execution and First Results, *J. Geophys. Res.*

Jordan, C. E., Anderson, B. E., Talbot, R. W., Dibb, J. E., Fuelberg, H. E., Hudgins, C. H., Kiley, C. M., Russo, R., Scheuer, E., Seid, G., Thornhill, K. L., and Winstead, E. (2003a). Chemical and Physical Properties of Bulk Aerosols

Within Four Sectors Observed during TRACE‐P, *J. Geophys. Res.* 108(D21):GTE 34-1–GTE 34-19.

Jordan, C. E., Dibb, J. E., Anderson, B. E., and Fuelberg, H. E. (2003b). Uptake of Nitrate and Sulfate on Dust Aerosols during TRACE-P, *J. Geophys. Res.* 108 (D21):GTE 38-1–GTE 38-10.

Liu, B.Y.H., Pui, D. Y. H., Wang, X. Q., and Lewis, C. W. (1983). Sampling of Carbon Fiber Aerosols, *Aerosol Sci. Technol.*2:499–511.

Maring, H., Savoie, D. L., Izaguirre, M. A., McCormick, C., Arimoto, R., Prospero, J. M., and Pilinis, C. (2000). Aerosol Physical and Optical Properties and their Relationship to Aerosol Composition in the Free Troposphere at Izaña, Tenerife, Canary Islands during July 1995, *J. Geophys. Res.* 105:14:667–14,700.

Moore, K. G., Clarke, A. D., Kapustin, V. N., and Howell, S. G. (2003). Long-Range Transport of Continental Plumes Over the Pacific Basin: Aerosol Physiochemistry and Optical Properties during PEM-Tropics A and B, *J. Geophys. Res.* 108(D2):PEM 8-1–PEM 8-27.

Moore, K. G., Clarke, A. D., Kapustin, V. N., McNaughton, C., Anderson, B. E., Winstead, E. L., Weber, R., Ma, Y., Lee, Y. N., Talbot, R., Dibb, J., Anderson, T., Doherty, S., Covert, D., and Rogers, D. (2004). A Comparison of Similar Aerosol Measurements Made on the NASA P3-B, DC-8, and NSF C-130 Aircraft during TRACE-P and ACE-Asia, *J. Geophys. Res.* 109(D3): 1–35.

Murphy, D. M., and Schein, M. E. (1998). Wind Tunnel Tests of a Shrouded Aircraft Inlet, *Aerosol Sci. Technol.*, 28 (1):33–39.

Peters, T. M., Chein, H., Lundgren, D. A., and Keady, P. B. (1993). Comparison and Combination of Aerosol Size Distributions Measured with a Low Pressure Impactor, Differential Mobility Particle Size, Electrical Aerosol Analyzer and Aerodynamic Particle Sizer, *Aerosol Sci. Technol.*, 19(3):396–405.

Porter, J. N., Clarke, A. D., Ferry, G., and Pueschel, R. F. (1992). Aircraft Studies of Size-Dependent Aerosol Sampling Through Inlets, *J. Geophys. Res.* 97(D4):3815–3824.

Raes, F., Dingenen, R. V., Vignati, E., Wilson, J., Putaud, J. P., Seinfeld, J. H., and Adams, P. (2000). Formation and Cycling of Aerosols in the Global Troposphere, *Atmos. Environ.* 34:4215–4240.

Ramanathan, V. E. A. (2001). The Indian Ocean Experiment: An Integrated Assessment of the Climate Forcing and Effects of the Great Indo-Asian Haze, *J. Geophys. Res.* 106 (D22): doi:10.1029/2001JD900133.

Raper, J. L., Kleb, M. M., Jacob, D. J., Davis, D. D., Newell, R. E., Fuelberg, H. E., Bendura, R. J., Hoell, C., and McNeal, R. J. (2001). Pacific Exploratory Mission in the tropical Pacific: PEM-Tropics B, March-April 1999, *J. Geophys. Res.*, 106 (D23):32,401–32,425.

Reid, J. S., Brooks, B., Crahan, K. K., Hegg, D. A., Eck, T. F., N. O'Neill, G. de Leeuw, Reid, E. A., and Anderson, K. D. (2006). Reconciliation of Coarse Mode Sea-Salt Aerosol Particle Size Measurements and Parameterizations at a Subtropical Ocean Receptor Site, *J. Geophys. Res.*, 111:D02202, doi: 10.1029/2005JD006200.

Reid, J. S., Jonsson, H. H., Maring, H. B., Smirnov, A., Savoie, D. L., Cliff, S. S., Reid, E. A., Livingston, J. M., Meier, M. M., Dubovik, O., and Tsay, S. C. (2003a). Comparison of Size and Morphological Measurements of Coarse Mode Dust Particles from Africa, *J. Geophys. Res.* 108 (D19):PRD 9-1–PRD 9-28.

Reid, J. S., Kinney, J. E., Westphal, D. L., Holben, B. N., Welton, E. J., Tsay, S., Eleuterio, D. P., Campbell, J. R., Christopher, S. A., Colarco, P. R., Jonsson, H. H., Livingston, J. M., Maring, H. B., Meier, M. L., Pilewskie, P., Prospero, J. M., Reid, E. A., Remer, L. A., Russell, P. B., Savoie, D. L., Smirnov, A., and Tanré, D. (2003b). Analysis of Measurements of Saharan Dust by Airborne and Ground-based Remote Sensing Methods during the Puerto Rico Dust Experiment (PRIDE), *J. Geophys. Res.* 108 (D19):PRD 2-1–PRD 2-27.

Rogers, R. R., and Yau, M. K. (1989). *A Short Course in Cloud Physics, 3rd ed.* Butterworth-Heinemann.

Sheridan, P. J., and Norton, R. B. (1998). Determination of the Passing Efficiency for Aerosol Chemical Species Through a Typical Aircraft-Mounted, Diffuser-Type Aerosol Inlet System, *J. Geophys. Res.* 103(D7):8215, 98JD00286.

Talbot, R. W., Dibb, J. E., and Loomis, M. B. (1998). Influence of Vertical Transport on Free Tropospheric Aerosols Over the Central USA in Springtime, *Geophys. Res. Lett.* 25:1367–1370.

Tang, I. N., Tridico, A. C., and Fung, K. H. (1997). Thermodynamic and Optical Properties of Sea Salt Aerosols, *J. Geophys. Res.* 102 (D19):23269–23276.

Wendisch, M., Coe, H., Baumgardner, D., Brenguier, J. L., Dreiling, V., Fiebig, M., Formenti, P., Hermann, M., Kramer, M., Levin, Z., Maser, R., Mathieu, E., Nacass, P., Noone, B., Osborne, S., Schneider, J., Schutz, L., Schwarzenbock, A., Stratmann, F., and Wilson, J. C. (2004). Aircraft Partile Inlets State-of-the-Art and Future Needs, *Bulletin of the American Meteorological Society*, 85:89–91.

Wilson, J. C., Lafleur, B. G., Hilvert, H., Seabaugh, W. R., Fox, W. J., Brock, C. A., Huebert, B. J., Geseler, D. R., Muller, J., and Reeves, J. M. (2004). Function and Performance of a Low Turbulence Inlet for Sampling Super-Micron Particles from Aircraft Platforms, *Aerosol Sci. Technol.* 38: 790–802.

Zar, J. H. (1974). *Biostatistical Analysis*, Prentice Hall, Englewood Cliffs, NJ.

APPENDIX

In the preceding manuscript we evaluated, as a percent difference, the relative agreement between airborne and ground-based measurements of aerosol size distributions and their optical properties. Here we tabulate the results of two-tailed Student's *t-test* in order to evaluate whether or not the mean values measured aboard the DC-8 aircraft are statistically indistinguishable (H_o) or statistically distinct (H_a) from those measured at the ground stations for $\alpha = 0.05$.

The Student's *t-test* requires that the population being tested be normally distributed and that variances are equal. The *f-test* is used to test for equal variance and in many cases fails. However, with regard to deviations from non-normality the *t-test* is more robust than the *f-test* particularly when the test is two-tailed and when the sample population suffers from low sample numbers (Zar 1974). Because our test is two tailed and suffers from low sample numbers (after pooling the data) and since we do not know if aerosol light scattering/volume is normally distributed in the ambient environment, we feel that the *t-test* is the best measure of inter-platform agreement even when the data do not meet the *f-test* criteria. The use of non-parametric rank-sum tests, such as the Mann-Whitney test, did not obviate problems with the two-tailed Student's *t-test*.

With regard to low sample numbers we are confronted with the fact that calculated means and variances aboard the DC-8 and at the ground station are not equal in space or time. In order to compare the scattering values or the distributions we must compare them over similar airmass volumes. This is accomplished by using the ratio of the DC-8 true airspeed (TAS) to the wind speeds (WS) measured at the EDW and THD towers. In the manuscript this is referred to as the "integration time" for the ground-based measurements. During DICE this ratio was as low as 9:1 and as high as 60:1. At EDW the aircraft and the ground station data share a common time base of 5-seconds. Scattering data at THD is recorded at 60-second intervals while switching between "Total" and "Submicrometer" scattering every 5 minutes. Thus five 5-second aircraft measurements correspond to between 46 and 301, 5-second samples at the EDW tower but as few as eleven, 1-minute samples at the THD tower. Variability of aerosol properties at the EDW tower is high due to airmass heterogeneity at micrometeorological scales. The occasional sampling of large aerosols results in coefficients of variation at the EDW tower that are higher than those measured

aboard the aircraft. Consequently, when comparing the aircraft data to the tower data, acceptance of the Students *t-test* null hypothesis is more easily achieved. To be more accurate in our comparison, variability at the EDW tower should be "smeared" into five "pooled" data points (N_{pool} as opposed to N_{tot} in Tables A, B, D, E, and F). The coefficients of variation of the pooled EDW tower means are comparable to those measured aboard the aircraft. This operation is not performed on the THD data set as each data point is already a 1-minute average. The effect of pooling the data is to increase the frequency of acceptance for the *f-tests* (a test for equal variance) but decreases the number of aircraft passes that meet the *t-test* criteria (a test for equal means).

Appendix Tables A and B tabulate the results of two-tailed *t-tests* performed on the TSI model 3563 3-λ nephelometer scattering data during each aircraft pass. In Appendix Table C the mean and standard deviations of the aircraft data collected in the 50–150 meter altitude range during vertical profiles is compared to the EDW and THD tower values over this so called aircraft "dwell time." Since these results do not compare identical airmass volume, statistical analysis using the *t-tests* is not appropriate. Also contained in Appendix Table C are the mean and standard deviations of total and submicrometer light scattering measured at the THD tower during DICE flight 8 and the corresponding data from the 15-minute level leg flown "upwind" of the THD site. Differences between wind speed and wind direction measured at THD and those measured aboard the DC-8 values over the open ocean magnify sampling uncertainties. Therefore we feel a more rigorous statistical analysis is not warranted.

Appendix Table D compares supermicrometer aerosol volume measured behind each inlet by the TSI model 3321 APS. Appendix Table E compares filter-based aerosol chemistry measurements at the EDW tower to those measured behind the UNH inlet aboard the DC-8 as well as calculated mass from APS size distributions. Strictly speaking the filter-based chemistry measurements do not sample equivalent airmass volumes. This is a technical limitation of the technique and we include a statistical analysis for completeness noting that our estimate of dust mass being composed of 5% Ca^{2+} by weight is the best fit to the data and highly uncertain.

Appendix Table F compares supermicrometer scattering values calculated from the APS aerosol size distributions in order to evaluate how large particle losses affect our ability to calculate aerosol optical properties. Since supermicrometer light scattering was dominated by particles smaller than ~5 μm during DICE and since the 50% passing efficiency of the UH and UNH inlet is better than 4 μm, there is better relative agreement between airborne and ground-based calculations of light scattering than between measurements of supermicrometer aerosol volume.

TABLE A

Student's *t-test* comparing light scattering $\lambda = 550$ nm) measured aboard the NASA DC-8 behind the University of Hawai'i solid diffuser type inlet to the values measured on the air traffic control tower at Edwards Air Force Base using an omni-directional inlet during DICE.

DICE Flight No.	Platform	ID	N_{pool} (N_{tot})	Mean (Mm^{-1})	% Difference	Combined[1] Standard Deviation (Mm^1)	t-test Ho: $\mu 1 = \mu 2$ Ha: $\mu 1 \neq \mu 2$
	EDW	Pass #1	5(151)	42.3		1.7	
RF05	Tower	Pass #2	5(151)	43.8		1.5	
	UH DC-8	Pass #1	5	42.9	1.5%	0.5	Accept
	Inlet	Pass #2	5	42.9	−2.0%	1.0	Accept
	EDW	Pass #1	5(46)	32.2		0.6	
RF06	Tower	Pass #2	5(46)	35.1		0.8	
	UH DC-8	Pass #1	5	37.7	17.1%	6.8	Accept
	Inlet	Pass #2	5	35.3	0.7%	3.5	Accept
		Pass #1 corr.	3	33.4	3.7%	1.1	Accept
		Pass #2 corr.	4	33.8	−3.6%	1.2	Accept
	EDW	Pass #1	5(301)	49.9		0.8	
	Tower	Pass #2	5(301)	50.0		1.0	
		Pass #3	5(301)	28.5		1.5	
		Pass #4	5(301)	26.7		0.8	
		Pass #5	5(301)	25.5		0.9	
RF08		Pass #6	5(301)	24.3		1.0	
	UH DC-8	Pass #1	5	52.3	5.0%	0.7	Reject
	Inlet	Pass #2	5	50.0	0.0%	0.5	Accept
		Pass #3	5	29.1	2.2%	0.5	Accept
		Pass #4	5	26.9	0.7%	1.2	Accept
		Pass #5	5	26.0	2.3%	1.4	Accept
		Pass #6	5	24.2	−0.3%	1.2	Accept

[1]Computed as the square root of the sum of squares of the standard deviation of the mean and the TSI nephelometer uncertainty (0.4 Mm^{-1} for a 25 s sample).

TABLE B

Student's *t-test* comparing light scattering ($\lambda = 550$ nm) measured aboard the NASA DC-8 behind the University of Hawai'i solid diffuser type inlet to the values measured at the NOAA/CMDL observatory at Trinidad Head California during DICE.

DICE Flight No.	Platform	ID	N_{tot}	Mean (Mm^{-1})	% Difference	Combined[1] Standard Deviation (Mm^{-1})	t-test Ho: $\mu 1 = \mu 2$ Ha: $\mu 1 \neq \mu 2$
	THD	Total Pass #1	3	10.7		1.2	
RF07	Tower	Total Pass #2	4	9.9		0.5	
	UH DC-8	Total Pass #1	5	10.4	−3.2%	0.5	Accept
	Inlet	Total Pass #2	5	10.7	7.7%	0.5	Accept
	THD	Sub Pass #1	6	9.1		0.8	
	Tower	Sub Pass #2	6	6.2		0.7	
	UH DC-8	Sub Pass #1	5	7.7	−16%	0.6	Accept
	Inlet	Sub Pass #2	5	6.3	0.4%	0.5	Accept
	THD	Total Pass #1	14	23.8		0.3	
	Tower	Total Pass #2	12	23.7		0.3	
		Total Pass #3	12	23.6		0.4	
RF08		Total Pass #4	11	23.3		0.6	
	UH DC-8	Total Pass #1	5	20.6	−14%	0.5	Reject
	Inlet	Total Pass #2	5	20.0	−16%	0.5	Reject
		Total Pass #3	5	21.6	−8.5%	0.5	Reject
		Total Pass #4	5	20.6	−12%	0.4	Reject
	THD	Sub Pass #1	12	11.5		0.3	
	Tower	Sub Pass #2	14	11.7		0.3	
		Sub Pass #3	14	12.0		0.6	
		Sub Pass #4	12	12.4		0.5	
	UH DC-8	Sub Pass #1	5	14.8	29%	0.5	Reject
	Inlet	Sub Pass #2	5	14.0	20%	0.5	Reject
		Sub Pass #3	5	14.0	17%	0.5	Reject
		Sub Pass #4	5	14.4	16%	0.6	Reject

TABLE C

Total and submicrometer aerosol light scattering ($\lambda = 550$ nm) measured behind the UH solid diffuser inlet during vertical profiles compared to the EDW and THD towers. Aircraft means and standard deviations are for all data collected over the 50–150 meter altitude range. Tower means and standard devations are for the entire aircraft dwell time, i.e. the samples are not equivalent airmass volumes

Regime	Flight	Description	EDW/THD Tower N_1	DC-8 N_2	EDW/THD mean-X_1 (Mm^{-1})	DC-8 mean-X_2 (Mm^{-1})	EDW/THD stdev-σ_1 (Mm^{-1})	DC-8 stdev-σ_2 (Mm^{-1})	Percent difference DC-8: EDW
EDW	RF05	Profile	541	163	43	41	2.4	3.6	−5.4%
Dust	RF06	Profile	361	132	34	36	1.9	6.5	7.5%
		Profile Corrected	361	100	34	34	1.9	3.5	1.5%
	RF08	Profile #1	721	90	50	50	2.6	3.1	−0.5%
		Profile #2	841	198	26	22	2.6	5.1	−15%
THD	RF07	Total-upwind							
Sea salt		23:30:30−24:35:30	33	186	11	9.9	0.7	0.7	−5.6%
		Total-upwind 23:30:30−25:57:35	71	186	12	9.9	1.4	0.7	−16%
		Submicron-upwind 23:24:30−24:41:30	39	186	6.3	5.6	0.6	0.6	−11%
		Submicron-upwind 23:24:30−26:05:30	75	186	6.2	5.6	1.1	0.6	−9.2%
	RF08	Total-profile 18:05:00−18:56:00	27	401	24	25	0.6	2.8	4.8%
		Submicron-profile 18:05:00-18:56:00	30	401	12	15	0.6	1.3	28%

TABLE D
Student's *t-test* comparing APS aerosol aerodynamic volume measured aboard the NASA DC-8 to the values measured on the air traffic control tower at Edwards Air Force Base during DICE.

DICE Flight No.	Platform	ID	N_{pool} (N_{tot})	Mean (μm^{-3} cm^{-3})	% Difference	Measurement Standard Deviation (μm^{-3} cm^{-3})	Ho: $\mu 1 = \mu 2$ Ha: $\mu 1 \neq \mu 2$
RF06	EDW	Pass #1	5(46)	15		1.1	
	Tower	Pass #2	5(46)	19		1.1	
	UH DC-8	Pass #1	5	15	−0.2%	3.3	Accept
	Inlet	Pass #2	5	18	−9.0%	2.1	Accept
	LaRC DC-8	Pass #1	5	8.1	−47%	3.1	Reject
	Inlet	Pass #2	5	5.5	−72%	1.1	Reject
	UNH DC-8	Pass #1	5	11	−29%	2.6	Reject
	Inlet	Pass #2	5	10	−46%	1.8	Reject
RF08	EDW	Pass #1	5(301)	44		9.2	
	Tower	Pass #2	5(301)	46		7.9	
		Pass #3	5(301)	10		1.2	
		Pass #4	5(301)	8.9		0.6	
		Pass #5	5(301)	8.4		0.9	
		Pass #6	5(301)	8.0		1.1	
	UH DC-8	Pass #1	5	30	−33%	4.8	Reject
	Inlet	Pass #2	5	23	−49%	1.6	Reject*
		Pass #3	5	12	23%	1.7	Reject
		Pass #4	5	12	29%	2.1	Reject*
		Pass #5	5	9.8	16%	3.6	Accept#
		Pass #6	5	9.7	21%	3.6	Accept
	LaRC DC-8	Pass #1	5	18	−60%	4.7	Reject
	Inlet	Pass #2	5	16	−65%	4.6	Reject
		Pass #3	5	8.1	−20%	3.7	Accept
		Pass #4	5	6.0	−33%	1.2	Reject
		Pass #5	5	5.8	−31%	1.8	Reject#
		Pass #6	5	4.7	−41%	2.2	Reject
	UNH DC-8	Pass #1	5	23	−48%	2.3	Reject
	Inlet	Pass #2	5	21	−54%	7.5	Reject*
		Pass #3	5	11	13%	1.3	Accept
		Pass #4	5	9.4	5.5%	3.9	Accept*
		Pass #5	5	9.6	14%	5.0	Accept
		Pass #6	5	7.5	−5.3%	1.9	Accept

*Tower flybys where UH and UNH inlet were swapped.
#Tower flybys where UH and LaRC inlet were swapped.

TABLE E

Filter-based bulk aerosol chemistry measurements at the EDW tower compared to filters behind the UNH inlet aboard the DC-8 and to aerosol mass calculated from APS volume equivalent diameters behind the UH and UNH inlets using a sea salt density of 2.2 g cm^{-3} and a dust density of 2.6 g cm^{-3}.

Regime	Flight	Platform	N_{pool} (N_{tot})	Mean Aerosol Mass ($\mu g\ m^{-3}$)	Standard Deviation ($\mu g\ m^{-3}$)	*t-test* result
Marine	RF07	DC-8 UNH	3	5.7	1.2	
		UH APS	3 (242)	5.9	1.7	
		UNH APS	3 (242)	5.3	1.3	
	RF08	DC-8 UNH	4	8.7	1.1	
		UH APS	4 (332)	14	5.1	
		UNH APS	4 (332)	12	6.4	
Desert	RF08	EDW Tower	2	18	8.1	Accept
	morning	DC-8 UNH	2 (93)	12	0.4	Accept
		UH APS	2(93)	17	3.5	Accept
		UNH APS		15	3.3	
	RF08	EDW Tower	4	7.6	4.1	Accept
	Afternoon	DC-8	4	7.0	1.1	Accept
		UH APS	4 (176)	7.2	1.9	Accept
		UNH APS	4 (176)	6.1	1.8	

TABLE F

Comparison of EDW Tower APS and DC-8 APS supermicrometer aerodynamic volume and APS derived ($\lambda = 550$ nm, m = 1.53 - 0.006i.) light scattering for both the morning (high dust) and afternoon (low dust) test periods during DICE flight 8.

		APS supermicrometer aerosol volume ($\mu m^3\ cm^{-3}$)				APS derived supermicrometer light scattering (Mm^{-1})			
	N	Mean	Standard Deviation	Percent Difference	*t-test* Result	Mean	Standard Deviation	Percent Difference	*t-test* Result
Tower	5(301)	44	9.2			16	3.0		
	5(301)	46	7.9			16	3.3		
	5(301)	10	1.2			5.8	1.1		
	5(301)	8.9	0.6			5.4	1.0		
	5(301)	8.4	0.9			5.1	1.2		
	5(301)	8.0	1.1			4.8	1.2		
UH	5	30	4.8	−33%	Reject	14	2.2	−12%	Accept
	5	23	1.6	−49%	Reject*	12	0.3	−27%	Reject*
	5	12	1.7	23%	Reject	6.6	0.6	14%	Accept
	5	12	2.1	29%	Reject*	6.4	0.5	19%	Reject*
	5	9.8	3.6	16%	Accept#	5.4	1.2	6%	Accept#
	5	9.7	3.6	21%	Accept	5.4	1.2	12%	Accept
UNH	5	23	2.3	−48%	Reject	12	0.8	−27%	Reject
	5	21	7.5	−54%	Reject*	11	1.5	−32%	Reject*
	5	11	1.3	13%	Accept	6.4	0.5	10%	Accept
	5	9.4	3.9	5.5%	Accept*	5.4	1.0	1.2%	Accept*
	5	9.6	5.0	14%	Accept	6.6	3.7	29%	Reject
	5	7.5	1.9	−5.3%	Accept	4.8	0.5	−1.7%	Accept

*Tower flybys where UH and UNH inlet were swapped.

#Tower flybys where UH and LaRC inlet were swapped.